



SCHOOL of
GRADUATE STUDIES
EAST TENNESSEE STATE UNIVERSITY

East Tennessee State University
Digital Commons @ East
Tennessee State University

Electronic Theses and Dissertations

Student Works

8-2005

Cell Toxicity and Uptake of RRR-Alpha-Tocopheryl Polyethylene Glycol 1000 Succinate (TPGS) by Various Cell lines *In Vitro*.

Christelle Komguem Kamga
East Tennessee State University

Follow this and additional works at: <https://dc.etsu.edu/etd>

 Part of the [Organic Chemistry Commons](#)

Recommended Citation

Komguem Kamga, Christelle, "Cell Toxicity and Uptake of RRR-Alpha-Tocopheryl Polyethylene Glycol 1000 Succinate (TPGS) by Various Cell lines *In Vitro*." (2005). *Electronic Theses and Dissertations*. Paper 1040. <https://dc.etsu.edu/etd/1040>

This Thesis - Open Access is brought to you for free and open access by the Student Works at Digital Commons @ East Tennessee State University. It has been accepted for inclusion in Electronic Theses and Dissertations by an authorized administrator of Digital Commons @ East Tennessee State University. For more information, please contact digilib@etsu.edu.

Cell Toxicity and Uptake of RRR- α -Tocopheryl Polyethylene Glycol 1000 Succinate
(TPGS) by Various Cell Lines *In Vitro*

A thesis
presented to
the faculty of the Department of Chemistry
East Tennessee State University

In partial fulfillment
of the requirements for the degree
Master of Science in Chemistry

by
Christelle Komguem Kamga
August 2005

William L. Stone, Chair
Thomas T. -S. Huang
Mian Jiang

Keywords: TPGS, RRR- α -Tocopherol, α - tocopheryl succinate, RAW 264.7
Macrophages, Toxicity, Uptake, HPLC/ECD, *p*-HATS, Cancer

ABSTRACT

Cell Toxicity and Uptake of RRR-alpha-Tocopheryl Polyethylene Glycol 1000 Succinate (TPGS) by Various Cell Lines *In Vitro*

by

Christelle Komguem Kanga

This research focused on investigating and comparing the cytotoxicity and cellular uptake of RRR-alpha-tocopheryl polyethylene glycol succinate (TPGS) with that of alpha-tocopheryl succinate (α -TS). Both TPGS and α -TS are water-soluble forms of vitamin E with important clinical applications. Cytotoxicity assays with RAW 264.7 and LNCaP cells incubated overnight with TPGS or α -TS at concentrations $\geq 12.4 \mu\text{M}$ suggest that α -TS is more cytotoxic than TPGS. Macrophages were found to be more sensitive than LNCaP cells when treated with similar concentrations of α -TS. For both cell lines, most of the TPGS or α -TS taken up remained esterified after 24 hours. Our results suggest that cell death was due to TPGS and/or α -TS and not alpha-tocopherol. A *para*-hydroxyanilide of α -TS (*p*-HATS) that could be used to distinguish between cellular TPGS and α -TS was studied. It was found that *p*-HATS can be detected electrochemically and that it is hydrolyzed to α -TOH.

ACKNOWLEDGEMENTS

I wish to express my profound gratitude to Dr William Stone who was willing to mentor me and introduce me to the fascinating world of biomedical research. His high expertise in vitamin E and cancer researches, as well as his patience and kindness were invaluable. I also heartfully thank Dr Thomas Huang who has initiated a turning point in my life. His great wisdom, patience, and kindheartedness have impacted my academic career as well as my personal life. I express my sincere thankfulness to Dr Mian Jiang for his willingness to be a member of my committee, for reviewing my thesis, and for giving me information about HPLC. Great thanks to Dr John Hyatt for generously donating samples of *p*-HATS and *p*-HA and for his collaboration in the study of these compounds.

I am also thankful to Mrs. Min Qui and Hongsong for their kindness, patience, and support while introducing me to the biochemistry skills needed for this work.

I thank the Faculty and staff of the Chemistry Department at East Tennessee State University for giving me the opportunity to pursue my studies in a pleasant environment and for the great experience I had while teaching.

To the members of the Pediatrics and Internal Medicine Journal Club, I express my gratefulness for their great collaboration and their willingness to share their knowledge.

I am thankful to my friends and fellow Cameroonians who have always being of great moral support in good and bad times.

CONTENTS

	Page
ABSTRACT	2
ACKNOWLEDGEMENTS	3
LIST OF FIGURES	7
Chapter	
1. INTRODUCTION	10
Vitamin E Compounds.....	10
Natural Forms of Vitamin E	10
A Special Ester Derivative of Natural Alpha -Tocopherol: TPGS.....	12
Free Radicals	13
Oxidative Stress and Antioxidants	15
Antioxidant Properties of Vitamin E	18
Cancer and Vitamin E.....	21
Cell Viability Assays and Cell Death	22
Theory of High Performance Liquid Chromatography Operation	24
A <i>Para</i> -Hydroxyanilide Derivative of RRR- α - Tocopheryl Succinate: <i>p</i> -HATS ...	27
2. METHODOLOGY	29
Reagents and Materials	29
Preparation of Solutions.....	30
Methods.....	32
Cell Viability Assays.....	32
Dyes Addition.....	33
PI Assay	34

CFDA Assay	34
MTT Assay.....	34
Cellular Uptake and Hydrolysis of TPGS and α -TS.....	35
Cell Lysate Preparation.....	36
Addition of Ethanol and Antioxidants	36
Extraction	36
Measurement of Tocopherol Using HPLC/ECD.....	37
Response Factor Determination	37
Properties of <i>p</i> -HATS.....	38
3. RESULTS	39
Cytotoxicity of TPGS and α -TS	39
Determination of Optimal PI and CFDA Concentrations in Cell Viability Assays.....	39
Selection of Optics for Fluorescence Readings	41
Dose-and Time-Dependent Viability of RAW 264.7 Macrophages Treated With TPGS.....	43
Comparative Viability of RAW 264.7 and LNCaP Cells Treated With TPGS.....	47
Comparative Viability of RAW 264.7 and LNCaP Cells Treated With α -TS.....	48
Cellular Uptake of TPGS and α -TS.....	49
Dose-Dependent Uptake and Hydrolysis of TPGS and α -TS	49
Time-Dependent Uptake and Hydrolysis of TPGS.....	55
Concentration Calibration Curves of α -TOH and 5, 7-DMT	56
Properties of <i>p</i> -HATS	58
Oxidation Potential for Electrochemical Detection of <i>p</i> -HATS.....	58

Retention Time of <i>p</i> -HATS Relative to 5, 7-DMT	59
Retention Time of <i>p</i> -HA relative to 5, 7-DMT.....	60
Extraction of <i>p</i> -HATS	61
Hydrolysis of <i>p</i> -HATS	66
4. DISCUSSION	69
5. CONCLUSION	72
BIBLIOGRAPHY	73
APPENDIX.....	75
VITA.....	78

LIST OF FIGURES

Figure	Page
1. Structures of Naturally Occurring Forms of Vitamin E	11
2. Chemical Structure of TPGS	12
3. Reduction of Molecular Oxygen to Water	14
4. Structure of EDTA	16
5. Structures of Pyrogallol and BHT	16
6. Structures of Some Naturally Occurring Antioxidants	17
7. Reaction Steps in Fatty Acids Autoxidation	18
8. Reaction of an α -Tocopherol Molecule with a Fatty Acid Peroxyl Radical	19
9. Resonance Stabilization of Tocopheroxyl Radical	19
10. Regeneration of α -Tocopherol Mediated by L-Ascorbic Acid	20
11. Regeneration of α -Tocopherol Mediated by Ubiquinol	21
12. Chemical Structure of 3-(4, 5-Dimethylthiazol-2-yl)-2, 5-Diphenyltetrazolium Bromide (MTT)	23
13. Chemical Structure of Propidium Iodide (PI)	23
14. Structures of 5, 6-Carboxyfluorescein Diacetate and 5, 6-Carboxyfluorescein	24
15. Chemical Structure of Rac-5, 7-Dimethyltocol	25
16. Components of the HPLC System	26
17. The Elution Order of Rac-5, 7- DMT and α -Tocopherol in Reversed Phase HPLC ..	27
18. Chemical Structure of <i>p</i> -HATS	27
19. Structure of <i>p</i> -HA	28
20. Experimental Design in Cell Viability Study	32

Figure	Page
21. Layout of the 96-Well Plate in Dose-Dependent Cell Viability Assays	33
22. Plate Layout in Time-Dependent Experiments.....	34
23. Diagram of Experimental Design for Measurement of Cellular Tocopherol Content	35
24. Determination of the Optimum PI Concentration	39
25. Determination of the Optimum CFDA Concentration	40
26. The Percentage of Dead Cells after 20 Hours of Incubation with Various Concentrations of Staurosporine	42
27. PI Assay of RAW 264.7 Macrophages Viability after 24 Hours of Incubation with Increasing Concentrations of TPGS-Enriched Medium	43
28. RAW 264.7 Macrophages Viability after 24 Hours of incubation with TPGS, as Measured by the CFDA Assay	44
29. RAW 264.7 Macrophages Viability as Measured with the MTT Assay after 24 Hours Incubation with TPGS	45
30. Time-Dependent CFDA Assay for RAW 264.7 Macrophages Viability after Incubation with 24.8 μ M TPGS	46
31. MTT Assay of RAW 264.7 and LNCaP Cells Incubated with TPGS for 24 Hours	47
32. MTT Assay of RAW 264.7 and LNCaP Cells Incubated with α -TS for 24 Hours ...	48
33. Cellular Concentration of Free Tocopherol after 24 Hours Incubation with TPGS ..	50
34. Cellular Concentration of Total Tocopherol in RAW 264.7 and LNCaP Cells after 24 Hours Incubation with TPGS	51
35. Cellular Concentration of Total Tocopherol after 24 Hours of Incubation With α -TS	52

Figure	Page
36. Cellular Concentration of Free Tocopherol after 24 Hours of Incubation With α -TS	53
37. Linear Relationship between Optical Density and Concentration for 5, 7-DMT	57
38. Linear Relationship between Optical Density and Concentration for α -TOH	57
39. Absolute Peak Areas of <i>p</i> -HATS as a Function of Oxidation Potential	58
40. Chromatogram of a Mixture of <i>p</i> -HATS and 5, 7-DMT in Mobile Phase	59
41. Chromatogram of a Solution of <i>p</i> -HA and 5, 7-DMT in Mobile Phase	60
42. Detector Signal as a Function of Retention Time for a Solution of 750 Pmol <i>p</i> - HATS and 288 Pmol 5, 7-DMT in Mobile Phase	61
43. Chromatogram of a Solution of <i>p</i> -HATS Extracted into Hexane	62
44. Chromatogram of a Solution of <i>p</i> -HATS Extracted into Octane	63
45. Chromatogram of a Solution of <i>p</i> -HATS Extracted into Methylene Chloride	64
46. Chromatogram of a Solution of <i>p</i> -HATS Extracted into Ethyl Acetate	65
47. Chromatogram of a Saponified Solution of <i>p</i> -HATS after Extraction into Ethyl Acetate	66
48. Chromatogram of a Saponified Solution of <i>p</i> -HATS after Extraction into Hexane.....	67
49. Chromatogram of a saponified solution of <i>p</i> -HATS after extraction into hexane and addition of α -TOH	68

CHAPTER 1

INTRODUCTION

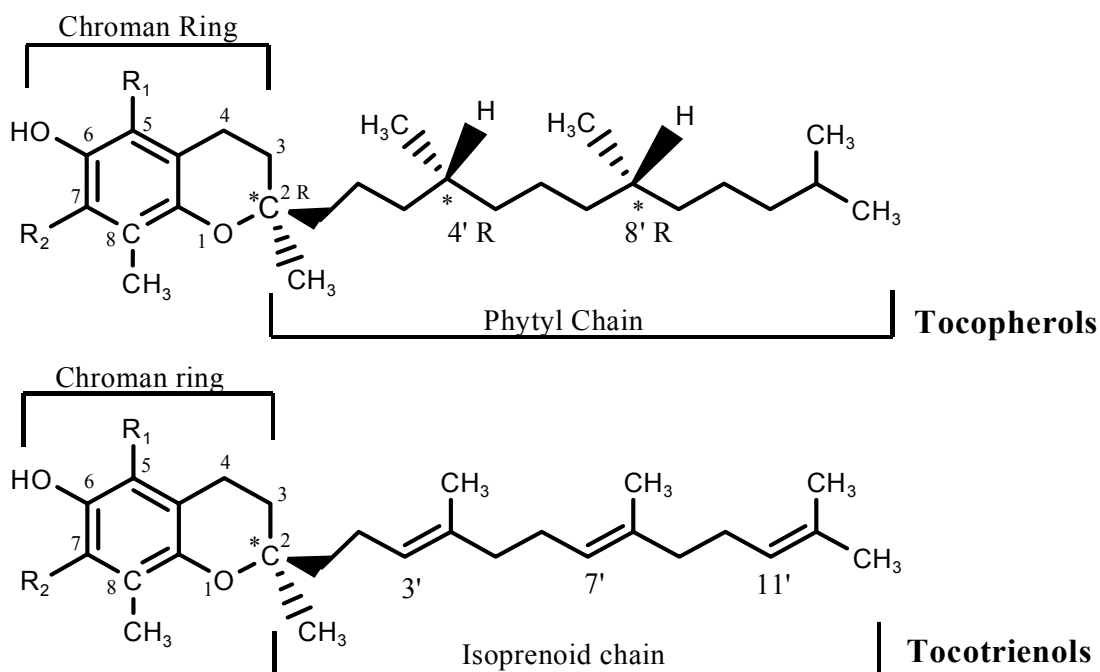
Vitamin E was labeled the ‘sex vitamin’ soon after its discovery in 1922 by Herbert Evans and Katharine Bishop, because of its important role in mammalian reproduction and fertility^{1,2}. After its lipophilic components, tocopherols and tocotrienols were isolated and characterized, research focused on vitamin E’s role as antioxidant². Vitamin E was shown to inhibit lipid peroxidation triggered by free radicals^{3,4}. Reactions of the latter with cellular components have been associated with the pathophysiology of some malignancies including cancers of the lungs, ovaries⁵, skin, prostate, colon⁶, stomach, and esophagus. Alpha-tocopherol, the predominant form of vitamin E in human and animal tissues, has been shown to scavenge lipid peroxy radicals, which are the chain-carrying species in lipid peroxidation^{2,3,4}. The antioxidant property of vitamin E suggests it might be a potential agent for tumor prevention^{7,8,9}.

In our study, we used RRR-alpha-tocopheryl polyethylene glycol 1000 succinate (TPGS), a water-soluble source of alpha-tocopherol for patients with fat malabsorption¹⁰. In this investigation, TPGS toxicity and uptake by different cell lines was studied in time and dose-dependent experiments. RAW 264.7 macrophage cells were used because they contain esterases that can hydrolyze TPGS. Studies were also carried out with androgen-dependent human prostate cancer cells (LNCAP).

Vitamin E Compounds

Natural Forms of Vitamin E

Vitamin E is a common name used to designate eight natural compounds of two types, tocopherols and tocotrienols. As the structures in Figure 1 show, these compounds all possess a chroman ring with different substitution patterns of methyl groups at positions 5 and 7 of the head group (α -, β -, δ -, γ -), and a 16-carbon side chain¹. However, while tocopherols have a saturated phytyl side chain with two chiral centers at carbons 4’ and 8’, tocotrienols possess an unsaturated side chain with double bonds at positions 3’, 7’, and 11’.



Compound	R ₁	R ₂
α-tocopherol/tocotrienol	CH ₃	CH ₃
β-tocopherol/tocotrienol	CH ₃	H
γ-tocopherol/tocotrienol	H	CH ₃
δ-tocopherol/tocotrienol	H	H

Figure 1. Structures of naturally occurring forms of Vitamin E. Chiral centers are indicated by an *.

Of all natural forms, α-tocopherol has the highest biological activity and is the predominant form of this vitamin found in human tissues¹. It also exists in a synthetic form. However, by virtue of the three chiral carbons at positions 2, 4' and 8', the synthetic all-racemic-α-tocopherol is a mixture of eight stereoisomers rather than a single compound¹. The natural configuration of RRR-α-tocopherol is 2R, 4'R; 8'R. Chemical structures of d-α-tocopherol stereoisomers are given in the appendix.

A Special Ester Derivative of Natural Alpha -Tocopherol: TPGS

Alpha-tocopherol can be esterified by reaction with acids to form α -tocopheryl acetate, succinate, linoleate, or nicotinate¹. In the body, enzymes called esterases remove these acids, liberating the active α -tocopherol. Further esterification of the acid group of RRR- α -tocopheryl succinate by polyethylene glycol 1000 (PEG 1000) produces RRR- α -tocopheryl polyethylene glycol 1000 succinate (TPGS), whose structure is shown in Figure 2. TPGS is amphipatic and, in contrast to other fat-soluble forms of vitamin E, is water-soluble and forms its own micelles. This unique property has been used clinically to supply Vitamin E to patients with poor production of bile and pancreatic enzymes⁸.

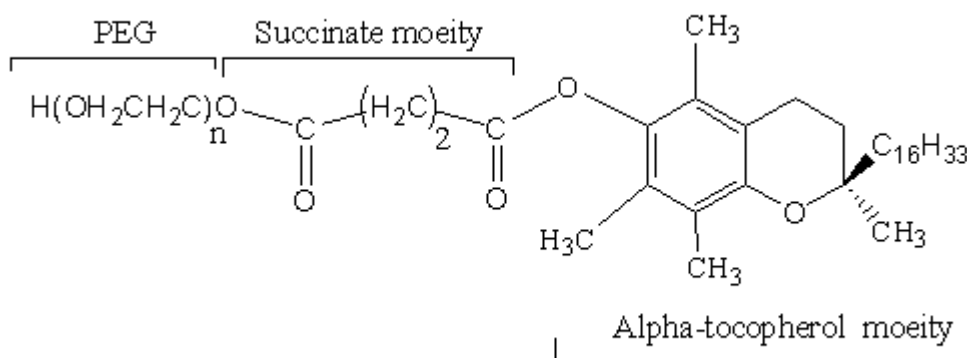


Figure 2. Chemical structure of TPGS. The diester has a polyethylene glycol group substituted at the carboxyl group of RRR- α -tocopheryl succinate. PEG stands for polyethylene glycol 1000.

TPGS hydrolysis would yield PEG and α -tocopheryl succinate (α -TS), and further hydrolysis of α -TS produces α -tocopherol (α -TOH) and succinate (S) as shown in equations (1) and (2). Alternatively, α -TOH, S, and PEG could directly be produced from TPGS by hydrolysis as given in equation (3).

Hydrolysis products of TPGS are:



Free Radicals

Free radicals are usually highly reactive chemical species carrying an odd, unpaired electron in their valence shell¹¹. They are generally unstable, short-lived, and capture an electron from another molecule to achieve stability. The molecule that loses its electron becomes a free radical itself, beginning a chain reaction. In vivo, free radicals can react with lipids, proteins, carbohydrates, and DNA. Damage caused by these reactions has been associated with the pathophysiology of several diseases such as cancer, arthritis, aging, and heart disease^{12, 13, 14}.

Oxyradicals result from the reduction of molecular oxygen¹¹. Reduction is a gain of electron(s) by a chemical species while oxidation is a loss of electron(s). The conversion of O₂ to H₂O involves a total gain of 4 electrons as depicted by the scheme in Figure 3. Intrinsically, the use of oxygen by aerobic organisms is associated with the risk of oxygen free radicals generation¹¹. Normal metabolic processes within the body (endogenous sources) that generate free radicals include phagocytosis, cell respiration, and oxygen transport between lungs and tissues. Exogenous sources of free radicals include ionizing radiations from industrial exhausts, sunrays, environmental pollutants such as ozone, and tobacco¹¹. Common examples of oxygen-derived damaging species are given in Table 1.

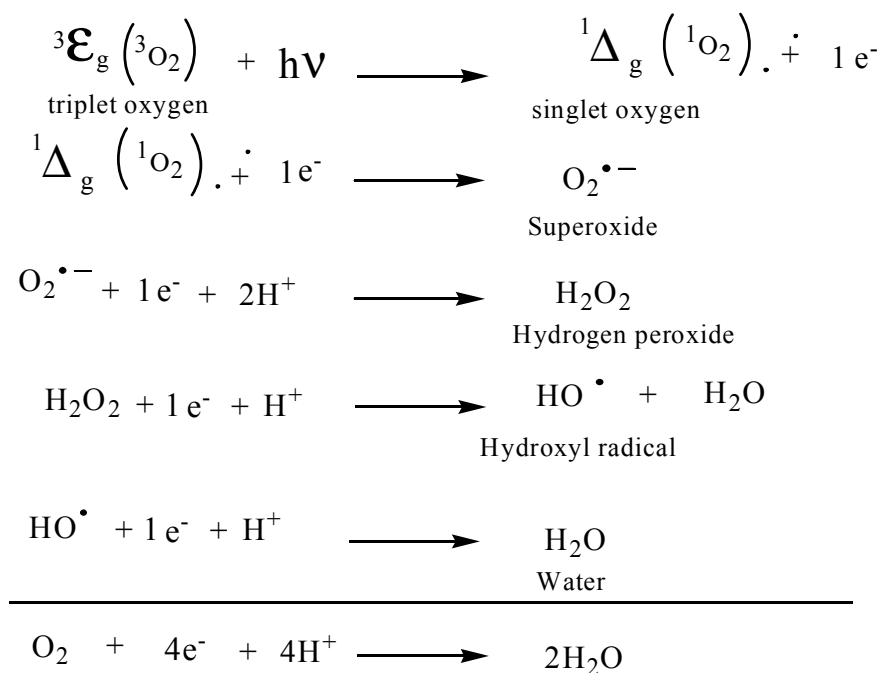


Figure 3. Reduction of molecular oxygen to water. It proceeds through steps that produce oxyradicals or their precursors.

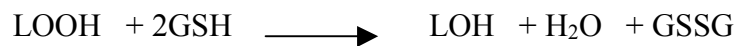
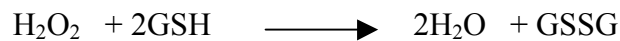
Table 1: Examples of oxygen-derived damaging species.

Radicals	Name	Non-radicals	Name
$\text{O}_2^{\bullet-}$	Superoxide radical	H_2O_2	Hydrogen Peroxide
HO^\bullet	Hydroxyl radical	${}^1\text{O}_2$	Singlet oxygen
ROO^\bullet	Peroxyl radical	HOCl	Hypochlorous acid
HO_2^\bullet	Hydroperoxyl radical	LOOH	Lipid hydroperoxide
LO_2^\bullet	Lipid peroxyl radical	O_3	Ozone

Oxidative Stress and Antioxidants

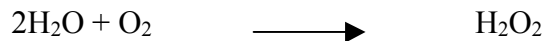
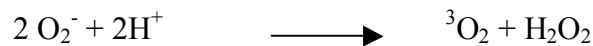
Oxidative stress is a physiological state that occurs when the generation of reactive oxygen species in a system exceeds the system's ability to neutralize and eliminate them¹⁵. Oxidation of various cellular components including DNA, lipids, and carbohydrates can lead to DNA damage, mitochondrial malfunction, cell membrane damage, and eventually cell death¹⁶. To suppress excessive oxyradicals and insure that tissues and metabolic processes can function properly, antioxidants are required. Antioxidants are substances that, when present in small amounts, inhibit reactions promoted by oxygen and/or free radicals. Antioxidants operate through four routes^{17, 18}:

- a) They break chain reactions: alpha-tocopherol breaks lipid peroxidation
- b) They decrease the concentration of reactive oxygen species : Glutathione peroxidase is an enzyme that removes H₂O₂ and lipid hydroperoxides (LOOH) as shown below:



GSH: Reduced glutathione GSSG: Oxidized glutathione

- c) They scavenge initiating radicals. Superoxide dismutase (SOD) traps superoxide radicals as shown below:



- d) They chelate transition metal catalysts. Ascorbic acid binds to transition metals.

Natural antioxidants include enzymes like catalase, glutathione peroxidase, superoxide dismutase (SOD), and glucose oxidase¹⁹. Vitamin E, ascorbic acid, carotenoids, flavonoids, and ubiquinol are other major chemical antioxidants. Antioxidants prepared synthetically include butylated hydroxytoluene (BHT), pyrogallol, and the metal chelator ethylene diamine tetra acetate (EDTA).

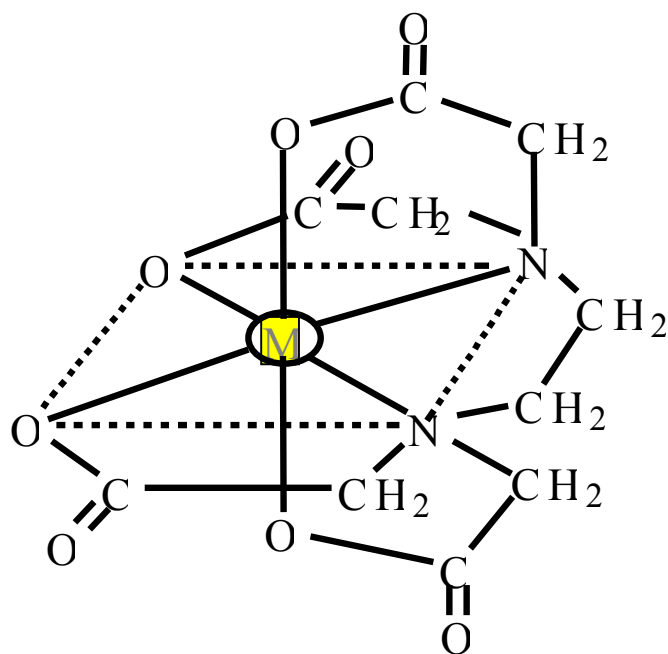
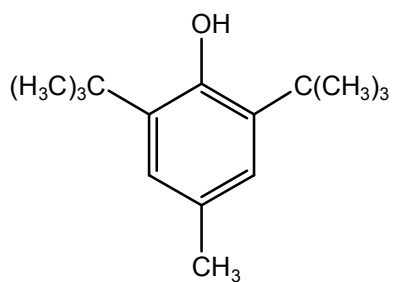
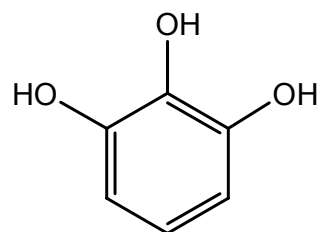


Figure 4. Structure of EDTA. The metal ion (M) is sequestered within the complex thereby preventing its redox cycling²⁰.



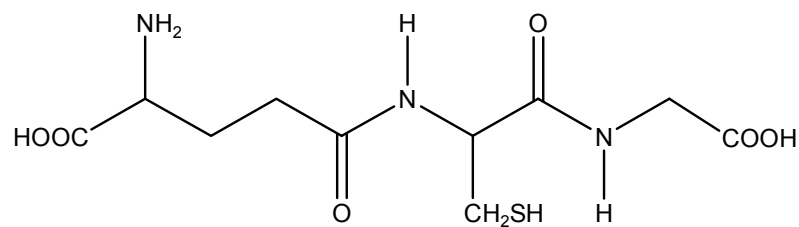
2,6-ditertiary-butyl-4-methyl phenol

BHT

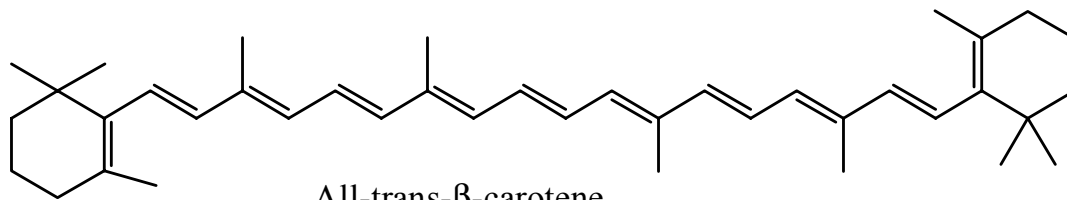


Pyrogallol

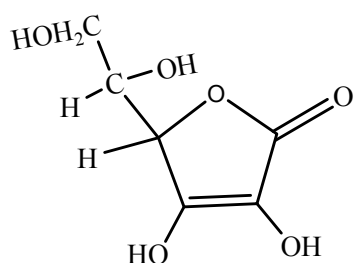
Figure 5. Structures of pyrogallol and BHT.



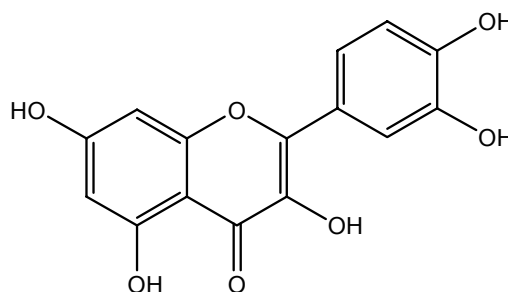
Glutathione(GSH)



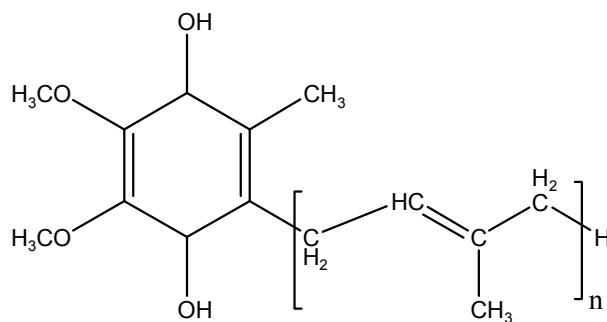
All-trans- β -carotene



L-Ascorbic acid (Vitamin C)



Quercetin (flavonoid)



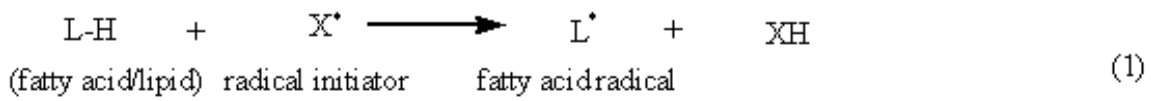
Ubiquinol

Figure 6. Structures of some naturally occurring antioxidants.

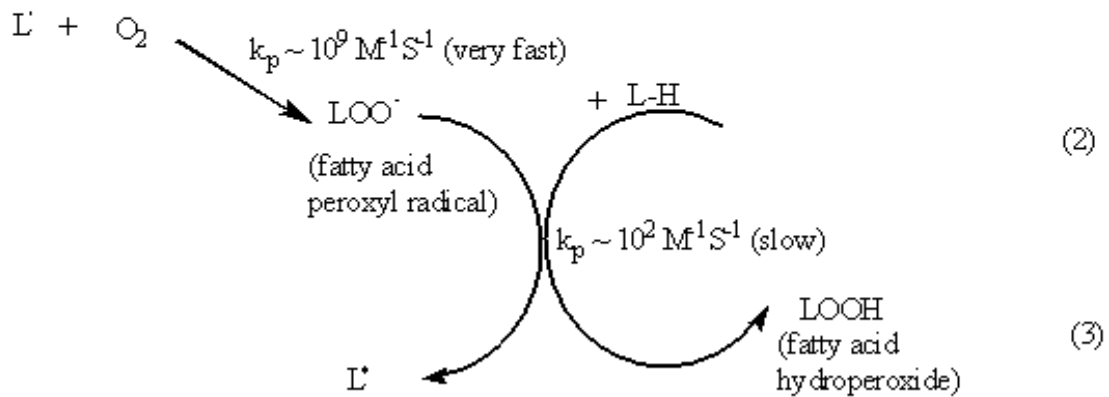
Antioxidant Properties of Vitamin E

Vitamin E compounds possess antioxidant properties due to the hydroxyl group at C6 of the chroman ring that can donate its hydrogen atom to terminate free radical chain reactions. One of the primary targets of free radicals in the body are polyunsaturated fatty acids (PUFA). They undergo a process called lipid peroxidation^{12, 13}. It has been experimentally shown that α-tocopherol acts as an antioxidant by scavenging lipid peroxy radicals (reaction 3 in Figure 7), which are the chain carrying species in lipid peroxidation. The steps involved in fatty acids autoxidation are summarized in Figure 7.

1) Initiation (Hydrogen removal)



2) Propagation (Autoxidation chain reaction)



3) Termination (Antioxidant reactions)

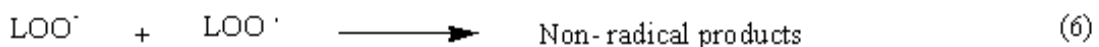
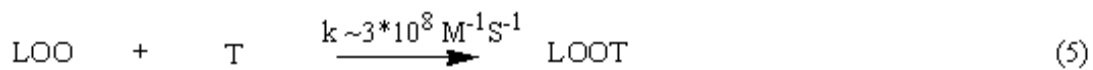
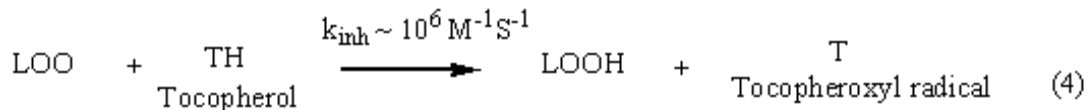


Figure 7. Reaction steps in fatty acids autoxidation.

The initiation step (reaction 1) is the abstraction of a hydrogen atom from the bis-allylic methylene of a PUFA by various agents including metal ions, UV and γ -radiations, and synthetic radical initiators²¹. The subsequent reaction (reaction 2) of the fatty acid radical with oxygen is exceedingly fast ($>10^9\text{M}^{-1}\text{s}^{-1}$) and produces a fatty acid peroxy radical. Chain propagation occurs when the peroxy radical removes a hydrogen atom from another fatty acid molecule (reaction 3). Encounter of the peroxy radical with a tocopherol molecule terminates the chain reaction (reaction 4)²². The tocopheroxyl radical formed is relatively stable due to the delocalization of the unpaired electron about the fully substituted chroman ring system²³.

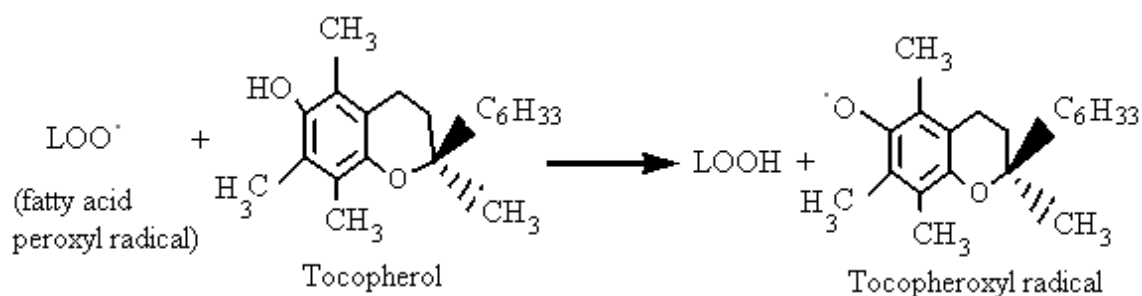


Figure 8. Reaction of an α -tocopherol molecule with a fatty acid peroxy radical.

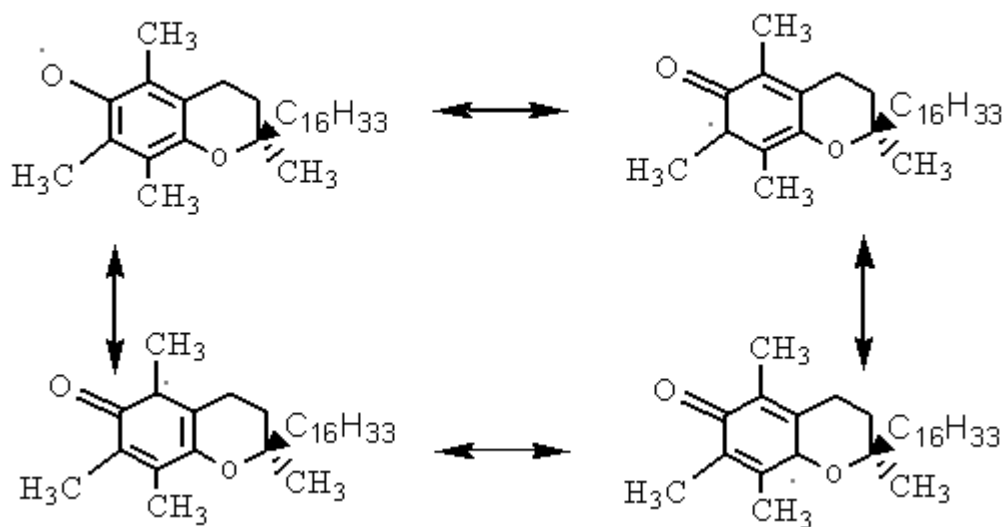


Figure 9. Resonance stabilization of tocopheroxyl radical.

The antioxidant potency of α -tocopherol is expressed by the relative rates of reactions (3) and (4) in Figure 7. The inhibition reaction is exceedingly fast compared to the propagation step. α -Tocopherol also reacts with singlet oxygen, ozone, alkoxy radicals, and superoxide. It can be observed from Table 2 that the peroxy radical has the lowest standard one-electron reduction potential among alkyl, alkoxy, and peroxy radicals. It is therefore the most prevalent target of Vitamin E compounds^{24, 25}.

Table 2. Standard one electron potential reduction for different redox systems.

Compounds	E^0 (mV)
$\text{HO}^\cdot, \text{H}^+/\text{H}_2\text{O}$	2310
$\text{RO}^\cdot, \text{H}^+/\text{ROH}$	1600
$\text{ROO}^\cdot, \text{H}^+/\text{ROOH}$	1000
$\text{PUFA}^\cdot, \text{H}^+/\text{PUFA}$	600
Catechol, $\text{H}^+/\text{Catechol}$	530
α -tocopheroxyl, H^+/α -tocopherol	500
ascorbate, $\text{H}^+/\text{ascorbate}$	282

The effectiveness of α -tocopherol as an antioxidant is further enhanced by its regeneration from its oxidized products. The recycling of α -tocopherol in vitro from its tocopheroxyl radical form, mediated by ascorbic acid and coenzyme Q, has been demonstrated to proceed as shown in Figures 10 and 11 below^{26, 27}:

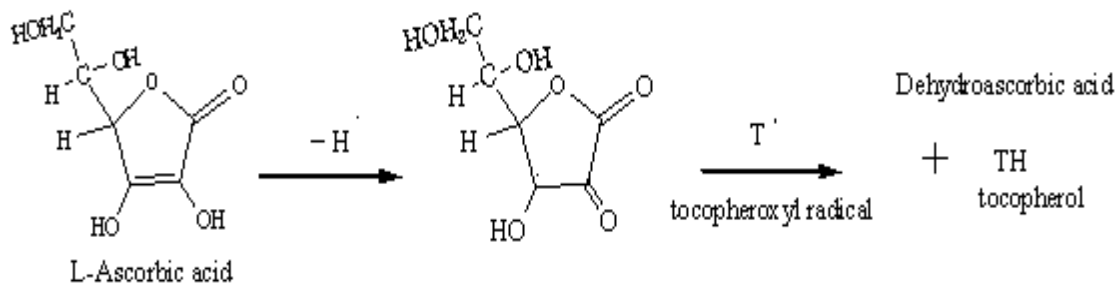


Figure 10. Regeneration of α -tocopherol mediated by L-ascorbic acid.

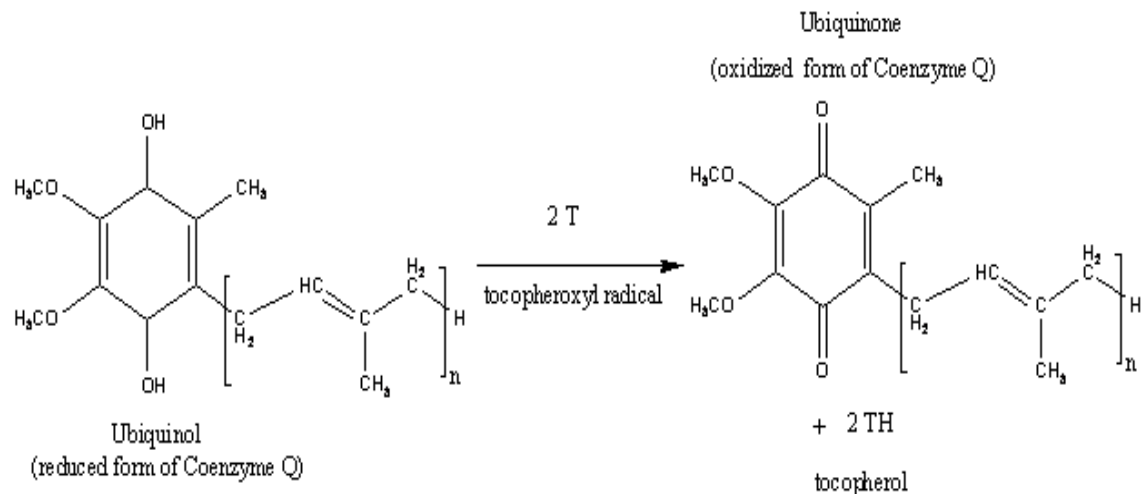


Figure 11. Regeneration of α -tocopherol mediated by ubiquinol.

Esters of α -tocopherol have a blocked hydroxyl group and therefore do not exhibit antioxidant function until the attached acid is removed by esterases in the body.

Cancer and Vitamin E

In recent years, cancer has surpassed heart disease as the leading cause of death among people under 85 in the US. More than a million new cancer cases are expected in 2005 with the main killer being lung cancer²⁸. Prostate cancer and breast cancers are the biggest killers among men and women respectively. Previous researchers have investigated the role of vitamin E homologues in helping fight and eventually prevent cancer.

High blood levels of α -tocopherol have been shown to cut the risk of prostate cancer by about 32% in clinical trials²⁹. In other experiments, α -tocopheryl succinate induced apoptosis in androgen-dependent human prostate cancer (LNCaP) cells without any effect on normal PrEC human prostate epithelial cells³⁰. However, to date, no study has been carried out on these cell lines with TPGS as a source of vitamin E. α -Tocopherol and α -tocopheryl succinate being two hydrolysis products of TPGS suggests the effects of this compound on cell lines are worthwhile investigating. In our study, the comparative toxicity and uptake of TPGS and α -tocopheryl succinate on RAW 264.7 macrophages and LNCaP cells were investigated.

Cell Viability Assays and Cell Death

Cell viability measurements are used to assess the number of healthy cells in a sample. This can be done either by counting the number of healthy cells directly using a hemocytometer or by measuring an indicator of cell growth. Two parameters are usually considered: metabolic activity or cell membrane integrity. An increase in cell viability indicates cell growth, whereas a decrease in viability might be a sign of a toxic substance or inadequate culture conditions.

Mitochondrial activity in cell populations was measured using 3-(4, 5-dimethylthiazol-2-yl)-2, 5-diphenyltetrazolium bromide (MTT). This is a salt that is reduced to blue-black formazan crystals in the mitochondria of live cells. It is therefore a measure of cell viability. Formazan crystals dissolve upon addition of an organic solvent like dimethyl sulfoxide (DMSO) to form a deep purple solution that absorbs light at 575 nm. Figure 12 shows the chemical structure of MTT.

Dye-exclusion assays take advantage of the ability of live cells with an intact cytoplasmic membrane to retain or exclude some dyes. The live cells population in samples was measured using a fluorophore called 5, 6-carboxyfluorescein diacetate (CFDA). This uncharged molecule penetrates into cell membranes and is converted in live cells by esterases to 5, 6-carboxyfluorescein, which as a dianion, is membrane impermeant. Only cells with intact plasma membranes retain the hydrolyzed form of the dye therefore accounting for the number of live cells. Carboxyfluorescein emits green fluorescence at wavelength 520 nm when excited at 485 nm.

Dye-exclusion assays can also be used to determine the population of dead cells in a sample. Propidium iodide (PI) is a membrane-impermeant dye that penetrates only into cells having a damaged plasma membrane and produces a red fluorescence upon binding to double-stranded nucleic acids and excitation at 485nm. It is completely excluded by live cells. The fluorescence signal emitted at 650 nm is directly proportional to the number of dead cells.

Cell death can occur by either of two distinct mechanisms: necrosis or apoptosis. Apoptosis sometimes referred to as “programmed” or “normal” cell death is the physiological process by which unwanted or useless cells are eliminated during growth and other normal biological processes. Necrosis, in contrast, occurs when cells are

exposed to extreme variance from physiological conditions, which may result in damage to the plasma membrane. It is therefore referred to as “accidental” cell death.

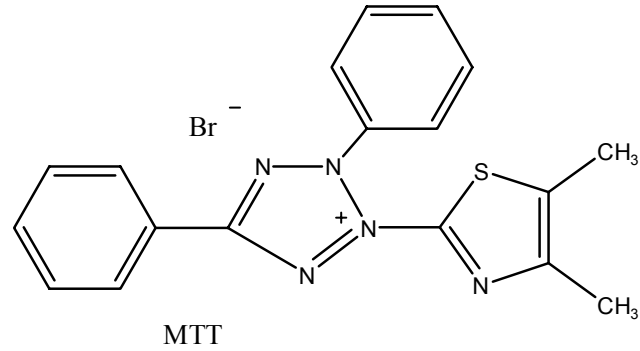


Figure 12. Chemical structure of 3-(4,5-dimethylthiazol-2-yl)-2,5-diphenyltetrazolium bromide (MTT).

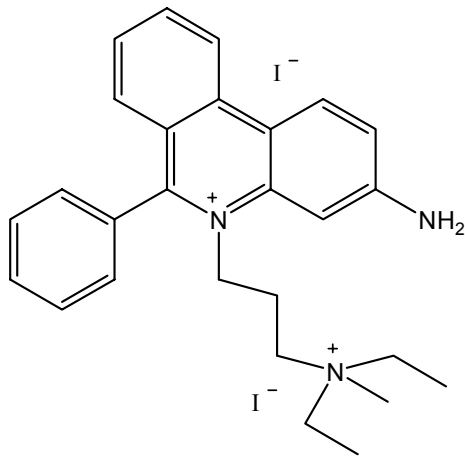


Figure 13. Chemical structure of propidium iodide (PI).

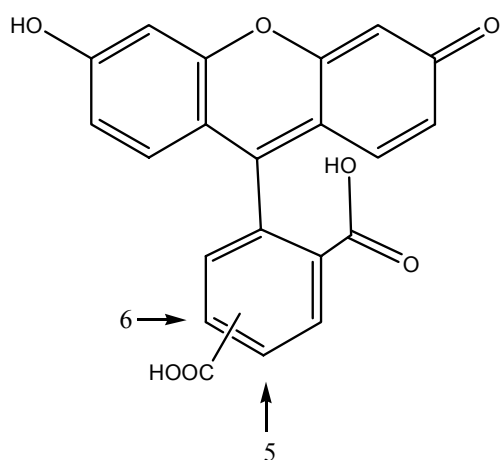
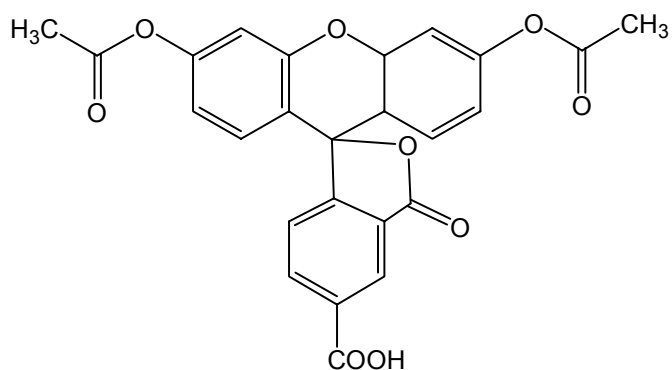


Figure 14. Structures of 5, 6-carboxyfluorescein diacetate and 5, 6-carboxyfluorescein.

Theory of High Performance Liquid Chromatography Operation

High performance liquid chromatography (HPLC) with electrochemical detection was used to measure α -tocopherol in samples. Chromatography is an analytical technique used to separate the components of a mixture based on their interaction with a stationary phase and a mobile phase. HPLC uses a liquid mobile phase (eluent) to carry the analytes through a column packed with a stationary material (adsorbent). The higher versatility of HPLC over other chromatographic techniques lies in the variety of eluents and adsorbents that can be used³¹. In adsorption chromatography, the active sites of the adsorbent interact with the functional groups of the analytes by noncovalent bonds, nonpolar interactions, Van der Waals forces, and hydrophobic interactions. Compounds less tightly

bound are eluted out by the mobile phase earlier and effective separation of classes of compounds can be achieved. There are two modes of adsorption chromatography based on the polarity of the phases: normal phase chromatography which uses a strongly polar adsorbent and a nonpolar mobile phase. The second mode is reversed-phase chromatography in which it is the inverse³¹.

In our study, reversed-phase chromatography was used and the internal standard was rac-5, 7-dimethyltocol (5, 7- DMT). An internal standard is a known amount of a compound, different from the analyte, which is added to the unknown³¹. Signal from the unknown is compared with that from the internal standard to find out how much analyte is present. Rac-5, 7-dimethyltocol was used as internal standard because its chromatographic and oxidation properties are similar to those of tocopherols. Figure 15 shows the structure of 5, 7-DMT.

Electrochemical detection was chosen as the detection method because it responds to electroactive substances and has high selectivity and sensitivity (picogram to femtogram level)³¹. The compound of interest is either oxidized (reduced) at a specific potential and the current (amperes) is proportional to the analyte concentration. When only a small fraction of the sample (5 to 15%) is oxidized (reduced) the detector is referred to as an amperometric detector. However, the entire sample can be oxidized (reduced) so that the signal is proportional to the total amount of the analyte in the injected sample. This type of detector is called coulometric and is generally more sensitive and stable than amperometric detection³¹. A diagram representing the main components of the HPLC system is shown in Figure 16.

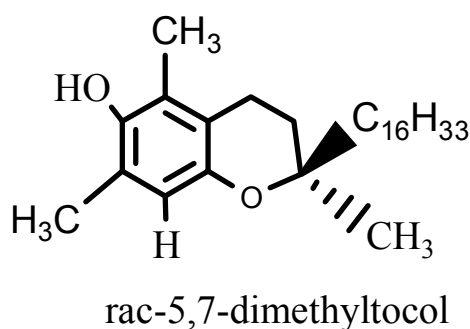


Figure 15. Chemical structure of rac-5, 7-dimethyltocol.

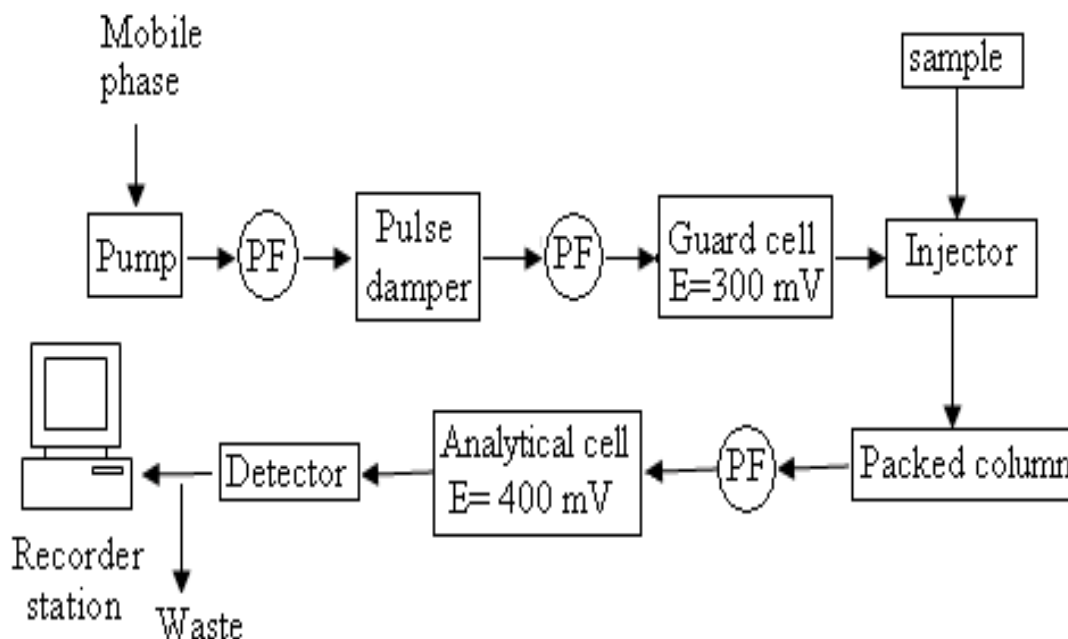


Figure 16. Components of the HPLC system. PF stands for prefilter³¹.

The constant flow pump delivers the mobile phase to the pre-filter where particulate impurities are removed. The pressure damper compensates for the pulsations in the eluent due to the pump action. The guard cell oxidizes (reduces) any electrochemically active material from the mobile phase. This reduces background current and baseline noise hence maximizing the sensitivity of the detector. The sample can be introduced into the mobile phase, without depressurizing the system, with the use of a microliter syringe and a loop-type injection valve. The detector emits a response due to each component eluting from the column and signals a peak on the chromatogram³¹.

In a sample containing rac-5, 7-dimethyltocol and α -tocopherol, the former elutes first because of its greater polarity. A sample of chromatogram showing the eluting positions of 5, 7-DMT and α -tocopherol in reversed-phase HPLC is represented in Figure 17.

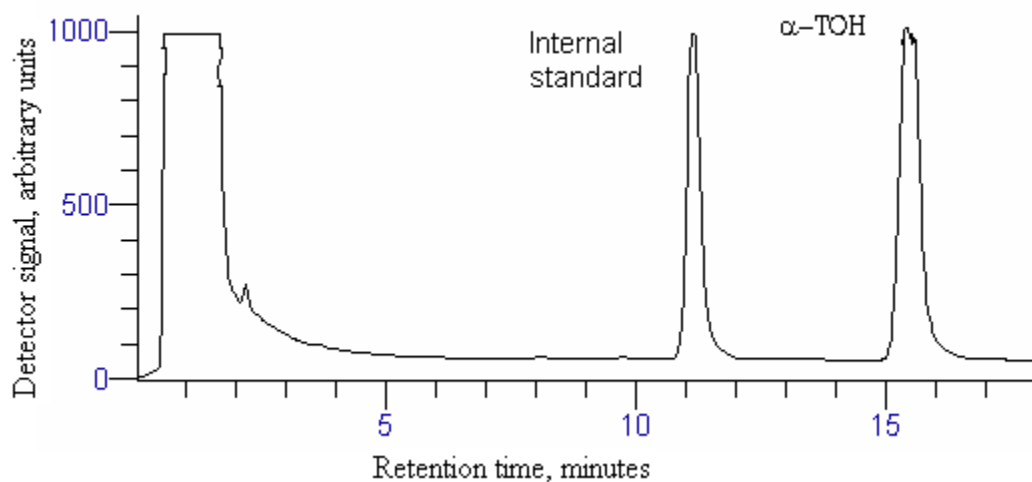


Figure 17. The elution order of rac-5, 7- DMT and α -tocopherol in reversed phase HPLC.

A *Para*-Hydroxyanilide Derivative of RRR- α -Tocopheryl Succinate: *p*-HATS

The last part of this study focused on the investigation of some critical properties of a compound referred to as *p*-HATS, which stands for *para*-hydroxyanilide of RRR- α -tocopheryl succinate. It has a molecular weight of 639 g/mol and is soluble in ethanol. The chemical structure of *p*-HATS is shown in Figure 18.

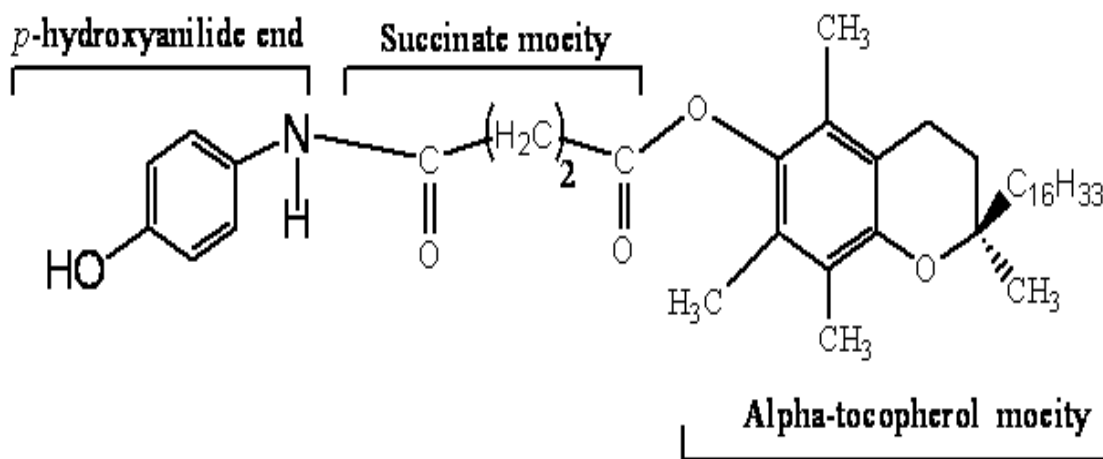


Figure 18. Chemical structure of *p*-HATS.

It can be noted from the structure in Figure 18 that the PEG 1000 end that exists in TPGS is replaced by *para*-hydroxyaniline. This makes *p*-HATS a very polar compound compared to TPGS. *p*-HATS also has a free hydroxyl group. Therefore, unlike α -TS, it is electroactive and can be detected by HPLC/ECD. This property could be used to measure the amount of α -TS in a sample used as a starting reagent for the synthesis of *p*-HATS. Therefore, it could be an analytical tool to determine the amount of α -TS in cellular systems using HPLC/ECD. The chromatographic properties of *p*-HATS, including the oxidation potential for its detection and its retention time relative to 5,7-DMT were investigated.

A by-product of *p*-HATS synthesis is *para*-hydroxyaniline (*p*-HA). Its chemical structure is shown in Figure 19 below.

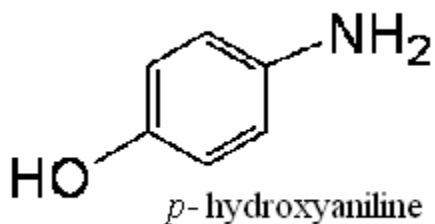


Figure 19. Structure of *p*-HA.

p-HATS is a diester. Its possible hydrolysis products include *p*-HA, α -TS, succinate, and α -TOH. Therefore, in addition to its ability to be detected by HPLC/ECD, it might be a potential source of α -TOH. As part of this research, a solvent appropriate for the extraction of *p*-HATS was determined and an attempt was made to determine the products of *p*-HATS hydrolysis.

CHAPTER 2

METHODOLOGY

Reagents and Materials

RAW 264.7 macrophages and LNCaP cells were purchased from American Type Culture Collection (Manassas, VA). RPMI-1640 medium with phenol red, fetal bovine serum (FBS), penicillin (10,000 units/ml), streptomycin (10,000 μ g/ml), dimethyl sulfoxide (DMSO), and 1x phosphate buffer saline (PBS) were purchased from Life Technologies (Grand Island, NY). TPGS was donated by Tennessee Eastman (Kingsport, TN), α -tocopherol succinate, α -tocopherol, *p*-HATS, and *p*-HA were synthesized and generously provided by Dr. John Hyatt. Rac-5, 7-dimethyl tocol was purchased from Matreya (Pleasant Gap, PA). Propidium iodide and 5, 6-carboxyfluorescein diacetate were purchased from Invitrogen Corporation (Carlsbad, CA). Pluronic acid, 3-(4, 5-dimethylthiazol-2-yl)-2, 5-diphenyltetrazolium bromide (MTT), Ethylene diamine tetra acetic acid (EDTA), citric acid, sodium hydroxide, butylated hydroxytoluene (BHT), ascorbic acid, pyrogallol, and Triton X-100 were purchased from Sigma Chemical Co. (St. Louis, MO). Hexane, methylene dichloride, and ethyl acetate were purchased from Fisher Scientific (Fair Lawn, NJ). Ethanol was purchased from Aaper Alcohol and Chemical Co. (Shelbyville, KY).

Costar 75 cm²/tissue culture flasks (sterile) and cell culture plates (sterile) were purchased from Costar (Cambridge, MA). Cell scrapers and pipettes were from Fisher Scientific (Fair Lawn, NJ). Syringe filters, (0.22 μ M and 0.45 μ M) purchased from Gelman Science (Ann. Arbor, MI).

Preparation of Solutions

Cell culture medium Prepared by mixing 450 mL of RPMI-1640, 50 mL of FBS, 2.5 mL of a 50mg/mL penicillin/streptomycin solution.

Polished water De-ionized water was filtered through a Sep-Pak cartridge (Water, Atlanta), and stored at 4°C.

NH₄OAc/HOAc buffer (pH=4.4) Ammonium acetate NH₄OAc (38.55 g) was dissolved in 500 mL of polished water. The pH was adjusted to 4.4 with acetic acid (HOAc) and stored at 4°C.

BHT solution in hexane 10ug/mL A 10.0 mg sample of BHT was dissolved in 1.0 liter hexane.

Citric acid solution (3.0 mM) 0.0288 g citric acid (MW=192.1 g/mol) was dissolved in polished water and diluted to a final aqueous volume of 50 mL and stored at 4°C.

Mobile phase used in HPLC/ECD An 80.0 mL aliquot of 1M NH₄OAc/HOAc buffer (pH=4.4) was mixed with 4.0 mL of 3.0 mM citric acid and polished water was added to give a final volume of 400 mL. The mixture was filtered through a 0.22 µm filter Millipore then mixed with 3600 mL of MeOH.

Mobile phase "Lite" polished water (400.0 mL) was filtered through a 0.22 µm filter Millipore then mixed with 3600 mL of HPLC grade MeOH.

Solution of BHT (220.36 g/mol) in 100% ethanol A mass of 0.0025 g BHT was dissolved in 100 mL of ethanol.

Ascorbic acid (176.1g/mol) solution: Prepared by dissolving 0.75 g in 5 mL of distilled water.

Pyrogallol (126.1 g/mol) solution: Prepared by adding 1.25 g of solid pyrogallol to 5 mL of ethanol.

Saturated KOH solution: KOH (14.508 g) was added to 10 mL of de-ionized water at room temperature.

Alpha-tocopheryl succinate (α-TS) stock solution: A mass of 0.0008 g α-TS (530.79 g/mol) was dissolved in 20 mL of ethanol.

Solutions of 5, 7-dimethyltocol: Working solutions were prepared from a 0.20 µM stock solution by dilution with ethanol.

Alpha-tocopherol solutions: A 10 mM stock solution was diluted with ethanol.

TRIS solution (0.2 M): A mass of 2.42 g was dissolved in 100 mL of distilled H₂O.

Triton X-100 solution (2% w/v): Prepared by dissolving 0.2 g of triton X-100 in 10 mL of distilled water.

EDTA tetra sodium (MW 380.2 g/mol) solution (1 M): Prepared by adding 3.80 g of EDTA to 10 mL of distilled water.

TPGS solutions: A stock solution (99.14 μ M) was prepared by dissolving 0.0075 g of TPGS (1513 g/mol) in 50 mL of boiling culture medium then the mixture was stirred for 2 hours and filtered through a 0.22 μ m filter. Working solutions were prepared by diluting the stock solution with culture medium.

Lysis buffer: A 10x solution was prepared by adding 20 mL of 0.2 M HCl and 25.0 mL of 0.2 M TRIS to a 50 mL graduated cylinder. Then, 2.5 mL of 2% triton X-100, 0.5 mL of 1 M EDTA solution, and 2.925 g of NaCl were added to the cylinder and the pH adjusted to 7.5. The total volume was brought to 50.0 mL with deionized water and the mixture filtered (Nalgene # 122-0045; 115 mL top bottle, 0.45 μ m pore size) and stored in 10 mL plastic bottles at -20° C. Prior to use, the lysis buffer was diluted 10-fold with deionized water.

PI solutions: A 1mg/ml stock solution was diluted with cell culture medium to the required working concentrations.

CFDA solutions: A 20% w/v Pluronic F-127/ DMSO solution was prepared by diluting 200 μ g of Pluronic F-127 in 800 μ L anhydrous DMSO and the solution was warmed gently at $\sim 40^{\circ}$ C. To 500 μ L of this mixture, 0.5 mg of CFDA (460 g/mol) was added. The final 2.17 mM stock solution was stored in molecular sieves.

MTT solutions: A 2.5 mg sample of MTT (335.43g/mol) was dissolved in 5 mL culture medium.

p-HATS solutions: A stock solution was prepared by dissolving 0.0016 g of solid p-HATS (639 g/mol) in 10 mL of ethanol. This was then diluted with ethanol for lesser concentrations.

p-HA solution: Prepared by dissolving 0.0025 g of solid p-HA (100 g/mol) in 10 mL of ethanol.

Methods

All cell lines were cultured in sterile flasks at 37°C in a humidified incubator with 95% air and 5% CO₂. After reaching confluence, they were seeded either in 96-well plates for cell viability studies or in 12-well plates for uptake analyses.

1. Cells were counted using a hemocytometer. They were then seeded into plates and incubated overnight.
2. Culture medium was removed and the vitamin E homologue (either TPGS or α -TS) working solution(s) added to the cells. Vitamin E solutions of different concentrations were used in dose-dependent experiments, at a single time-point. Different incubation periods were considered as a single concentration for time-dependent studies.

Cell Viability Assays

The three viability assays (PI, CFDA and MTT) were performed according to the scheme represented in Figure 20.

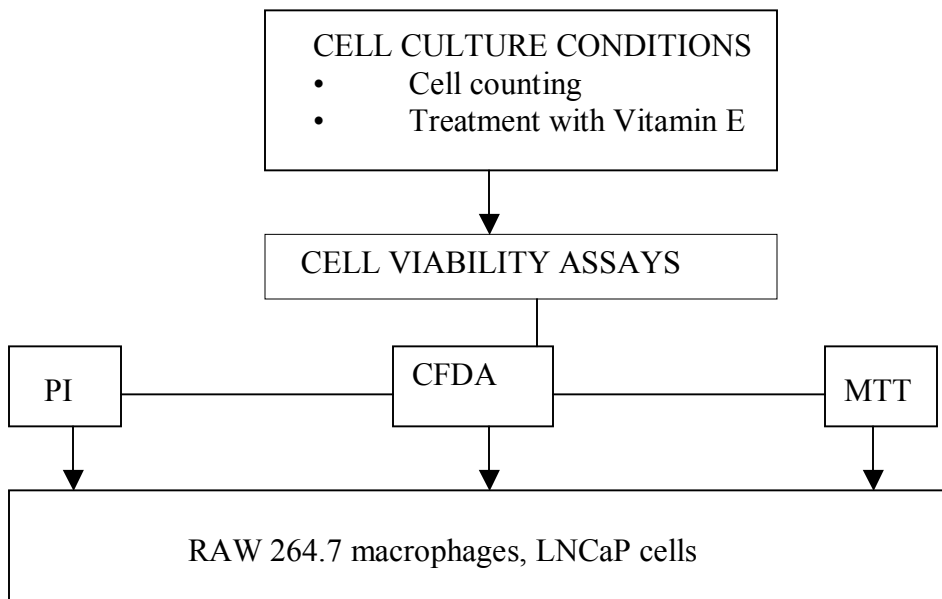


Figure 20. Experimental Design in Cell Viability Study.

Dyes Addition. After incubation with the vitamin E homologue solution(s), dyes were added. For each experiment all three assays were conducted in the same 96-well plate. Fluorescence was measured in PI and CFDA assays using a Fluostar Galaxy Microplate Reader from BMG Labtechnologies in the standard fluorescence configuration using bottom-bottom optics modes. Absorbance of samples was measured in MTT assays using a SpectraMax 190 Microplate Reader from Molecular Devices. Figure 21 shows the layout adopted for dose-dependent measurements.

C	C	C	C	C1	C1	C1	C1	C2	C2	C2	C2				
C3	C3	C3	C3	C4	C4	C4	C4	S	S	S	S				
C	C	C	C	C1	C1	C1	C1	C2	C2	C2	C2				
C3	C3	C3	C3	C4	C4	C4	C4	S	S	S	S				
C	C	C	C	C1	C1	C1	C1	C2	C2	C2	C2				
C3	C3	C3	C3	C4	C4	C4	C4	S	S	S	S				
B	B	B	B	B	B	B	B								

MTT
 CFDA
 PI

Figure 21. Layout of the 96-well plate in dose-dependent cell viability assays. The wells are labeled according to their contents. C: non-treated cells in culture medium, used as control. C1, C2, C3, and C4 are increasing concentrations of vitamin E homologues. S: cells treated with staurosporine, used as negative control. B: cells in medium that were not treated with a fluorophore, used as blank.

For time-dependent assays, slight modifications of the above layout were used. All wells contained cells treated with the same concentration of vitamin E. Increasing time points were represented as T1, T2, and T3. The blank used was the same as previously. Figure 22 shows the plate layout used in time-dependent experiments.

T1	T1	T1	T1	T2	T2	T2	T2	T3	T3	T3	T3
T1	T1	T1	T1	T2	T2	T2	T2	T3	T3	T3	T3
T1	T1	T1	T1	T2	T2	T2	T2	T3	T3	T3	T3
B	B	B	B	B	B	B	B				

MTT
 CFDA
 PI

Figure 22. Plate layout in time-dependent experiments.

PI Assay. A 100 μL aliquot of 3 μM PI was added to each well to give a final volume of 200 μL and a 1.5 μM PI concentration. The cells were incubated for 10 minutes with PI then the fluorescence measured (excitation 485nm/emission 650 nm).

CFDA Assay. Medium was first removed and cells washed three times with 1x PBS. A 100 μL aliquot of 1.1 μM CFDA was added to each well. After incubating for 10 minutes, fluorescence was measured (excitation 485 nm/emission 520 nm).

MTT Assay. Medium was first removed and 100 μL of the 0.5mg/mL MTT solution added to each well. Cells were incubated for 30 minutes for formation of blue formazan crystals. MTT was carefully removed from each well without disturbing the crystals and a 100 μL volume of DMSO added to dissolve them. Absorbance was measured at 570 nm after 30 minutes.

Cellular Uptake and Hydrolysis of TPGS and α -TS

An analytical method was devised to measure cellular uptake and hydrolysis of TPGS. Experiments were carried out using TPGS-treated cells and also with α -TS-treated cells. The experimental design used in this part of the study is shown in Figure 23.

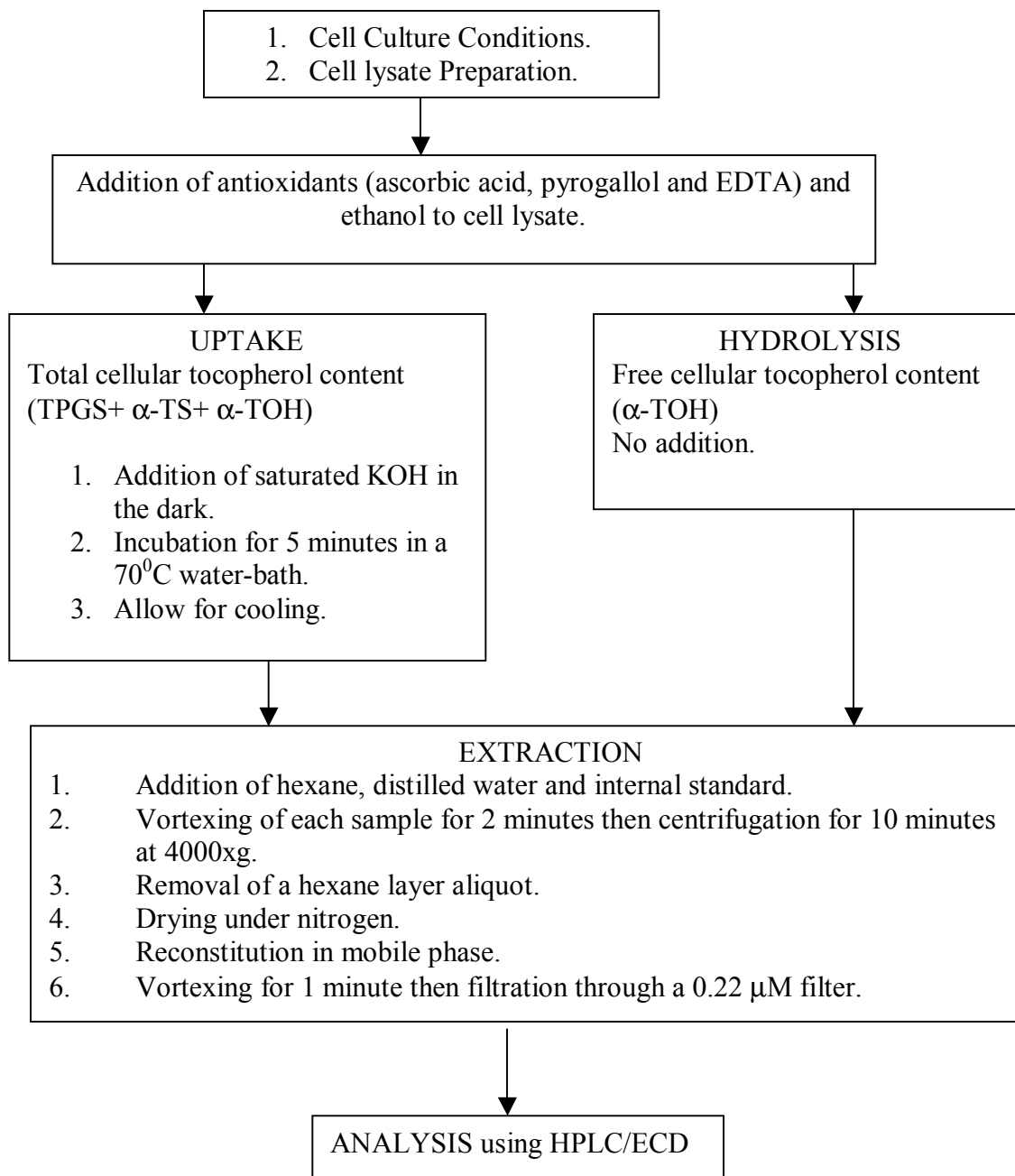


Figure 23. Diagram of experimental design for measurement of cellular tocopherol content.

Cell Lysate Preparation.

1. Cells were incubated in a 12-well plate with TPGS or α -TS. Time and dose-dependent experiments were carried out concurrently in the same well plate.
2. The medium was removed and the cells were washed three times with 1xPBS. They were overlaid with 1.5 mL of lysis buffer and scraped.
3. Cell lysate was collected in glass vials and submitted to two cycles of freezing and thawing.

Addition of Ethanol and Antioxidants. Cell lysate from each well was equally divided and put in two separate vials: one for the measurement of cellular total tocopherol and the other for free tocopherol. In separate glass vials, for every 500 μ L of cell lysate, 500 μ L of ethanol, 100 μ L of ascorbic acid, 100 μ L of pyrogallol, and 200 μ L of EDTA were added. To determine the total tocopherol content, the vial contents was hydrolyzed with saturated KOH as outlined in figure 21. Free tocopherol determination did not require any KOH hydrolysis.

Extraction. Both vials contents were then extracted into hexane. For every 500 μ L of initial cell lysate, 1 mL of hexane containing 10 μ g BHT, 250 μ L of distilled water and 250 μ L of rac-5, 7- dimethyl tocol as internal standard were added to each vial. The mixture was then vortexed for 2 minutes on a Maxi-Mix 1 mixer from BARNSTEAD/THERMOLYNE (Dubuque, IA). Samples were centrifuged for 10 minutes at 4000xg in an International Centrifuge from International Equipment Co. (Needham, MA). A 500 μ L aliquot of the supernatant hexane layer was removed from each vial and dried under nitrogen. A 200 μ L volume of mobile phase was then added and the mixture vortexed for 1 minute, filtered through a 0.22 μ m syringe-driven filter unit from Millipore Corporation (Billerica, MA), and either analyzed directly or kept at -20⁰C until used.

Measurement of Tocopherol Content Using HPLC/ECD. Cellular tocopherol content was measured using a HPLC equipped with a Coulochem II Electrochemical Detector, a ESA Model 580 Solvent Delivery Module, a HR-80 column(C 18, 3 μ m, 8 cm), a Model 5011 Analytical Cell, a Model 5020 Guard Cell (Chelmsford, MA), a PE Nelson 900 Series interface with PE Nelson Tuberschrom V4 Software (Perkin Elmer, San Jose, CA) using a Dell computer. Throughout the study, the flow rate was maintained at 1.5 mL/mn with E=300 mV, E2=400 mV. E and E2 are the potential of the guard cell and the analytical electrode, respectively.

Response Factor Determination. To use an internal standard, a known mixture of standard and analyte is prepared and the relative response of the detector to the two species carefully measured. Because α -tocopherol was the compound to measure, it was used to determine the response factor relative to rac-5, 7 -dimethyl tocol. Standard solutions of α -tocopherol and rac-5,7- dimethyl tocol were prepared and their maximum absorbance wavelengths measured using a Cary 50 Bio UV-Visible Spectrophotometer from Varian (Walnut Creek, CA). The standard solutions were mixed and the areas under the peaks measured by the HPLC/ECD method. Purity of 5, 7-DMT and α -TOH solutions was tested using HPLC with UV detection and the correction coefficients for concentrations obtained. The response factor F was determined as shown below:

A_T = area under the peak for α -TOH

A_{DMT} = area under the peak for rac-5, 7- DMT

[T] = concentration of α -TOH

[DMT]= concentration of rac-5, 7- DMT

The response factor F is given by the formula:

$$A_T / [T] = F \times (A_{DMT} / [DMT])$$

Once F is known, unknown concentrations of tocopherol can be obtained for subsequent sample runs, knowing [DMT], A_T and A_{DMT} .

$$[T] = (1/F) \times [DMT] \times (A_T/A_{DMT})$$

Properties of *p*-HATS

Pure solutions of *p*-HATS were prepared in ethanol. To determine the optimal oxidation potential for *p*-HATS detection, a mixture of 250 pmol *p*-HATS and 79 pmol of 5, 7-DMT was prepared in mobile phase. HPLC/ECD was used to detect both compounds at different oxidation potentials.

In order to determine a solvent suitable for the extraction of *p*-HATS, 500 μ L of a 25 μ M solution was treated with antioxidants. 5, 7-DMT was added and the extraction carried out into four different solvents: hexane, methylene chloride, octane and ethyl acetate. HPLC/ECD then used to detect *p*-HATS.

A solution of 120 pmol *p*-HA and 55 pmol 5, 7-DMT in mobile phase was prepared and analyzed using HPLC/ECD.

Saponification of 500 μ L of a 25 μ M *p*-HATS solution was carried out in order to identify the products of its hydrolysis. Extraction was done using hexane and ethyl acetate and the compounds detected by HPLC/ECD.

CHAPTER 3

RESULTS

Cytotoxicity of TPGS and α -TS

Determination of Optimal PI and CFDA Concentrations in Cell Viability Assays

RAW 264.7 macrophages were seeded in a 96-well plate, incubated overnight to adhere to the bottom of the wells, and then incubated with 2 μ M staurosporine (a positive control) for 16 hours. The population of dead cells was then evaluated using PI solutions of varying concentrations (0.15, 1.50, 3.70, and 6.00 μ M). Figure 24 shows the PI fluorescence as a function of the dye concentration.

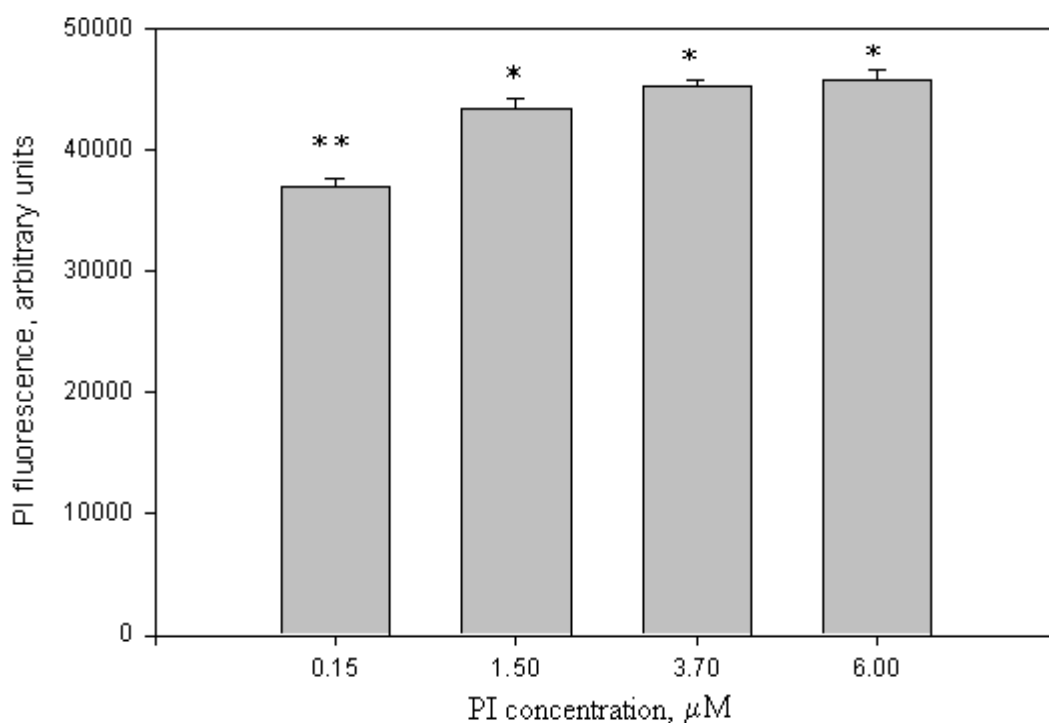


Figure 24. Determination of the optimum PI concentration. RAW 264.7 macrophages were treated with 2 μ M staurosporine for 16 hours. Cell viability was then assessed using different concentrations of PI. * Statistically different from 0.15 μ M PI and ** statistically different from other PI concentrations ($P < 0.05$). Values are means \pm S.E.M from 4 wells.

As shown in Figure 24, at PI concentrations above 1.50 μM , the strength of the fluorescence signal did not vary significantly with increasing PI concentrations. In all PI assays, 1.50 μM was therefore used.

CFDA has been shown to alter cell viability at high concentrations ($> 10 \mu\text{M}$)⁴¹. Therefore, in order to carry out an assay with this dye, a calibration must first be done in order to determine the minimum concentration that would produce high fluorescence in live cells. RAW 264.7 macrophages were seeded in a 96-well plate and left overnight to attach to the bottom of the wells. The medium was removed and cells washed 3 times with serum-free medium. CFDA solutions of concentrations 0.5, 1.1, 2.2, 3.5, and 4.3 μM were then used to assess the population of live cells.

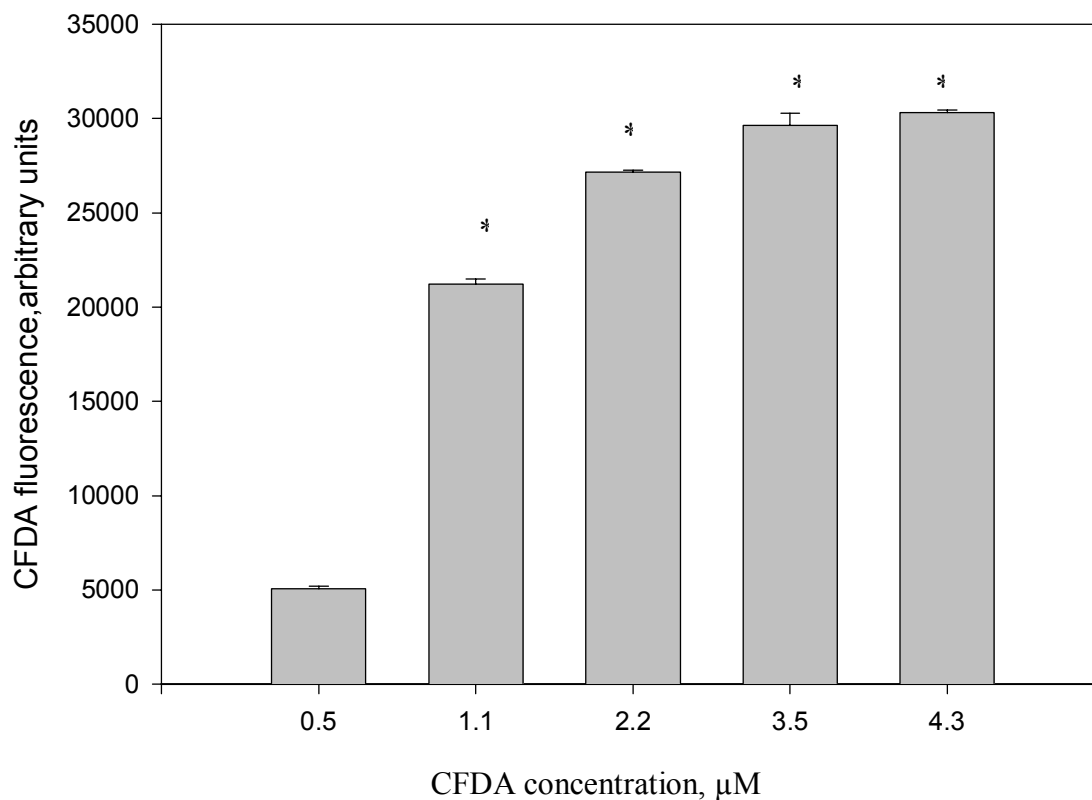


Figure 25. Determination of the optimum CFDA concentration. RAW 264.7 macrophages were seeded in a 96-well plate and left overnight to attach to the bottom of the wells. Cell viability was then assessed using different concentrations of CFDA. * Statistically different from 0.5 μM ($P < 0.05$). Values are means \pm S.E.M from 4 wells.

It is observed from Figure 25 that, above 1.1 μM , the fluorescence signal is high enough to indicate live cells populations; therefore, 1.1 μM was used in all CFDA assays.

Selection of Optics for Fluorescence Readings

On the Fluostar Galaxy microplate reader used for fluorescence measurements, it is possible to switch from top to bottom optics through a simple optical change. Cell-based assays are generally closer to the bottom optics, allowing more sensitive measurements. In order to determine the optimum optics settings in our study, a PI assay was carried out on cells incubated with 0.5 and 1.0 μM staurosporine for 20 hours. Readings from the four possible combination of optics (bottom-bottom, bottom-top, top-top, and top-bottom) are shown in Figure 26, along with results from an MTT assay. The percentage of dead cells relative to untreated cells was determined using the following formulae:

MTT assay

$$\% \text{ dead cells} = \{1 - (A_t/A_c)\} \times 100$$

PI assay

$$\% \text{ dead cells} = \{(F_t - F_c)/F_c\} \times 100$$

A_t = Absorbance of treated cells

A_c = Absorbance of control cells

F_t = Fluorescence of treated cells

F_c = Fluorescence of control cells

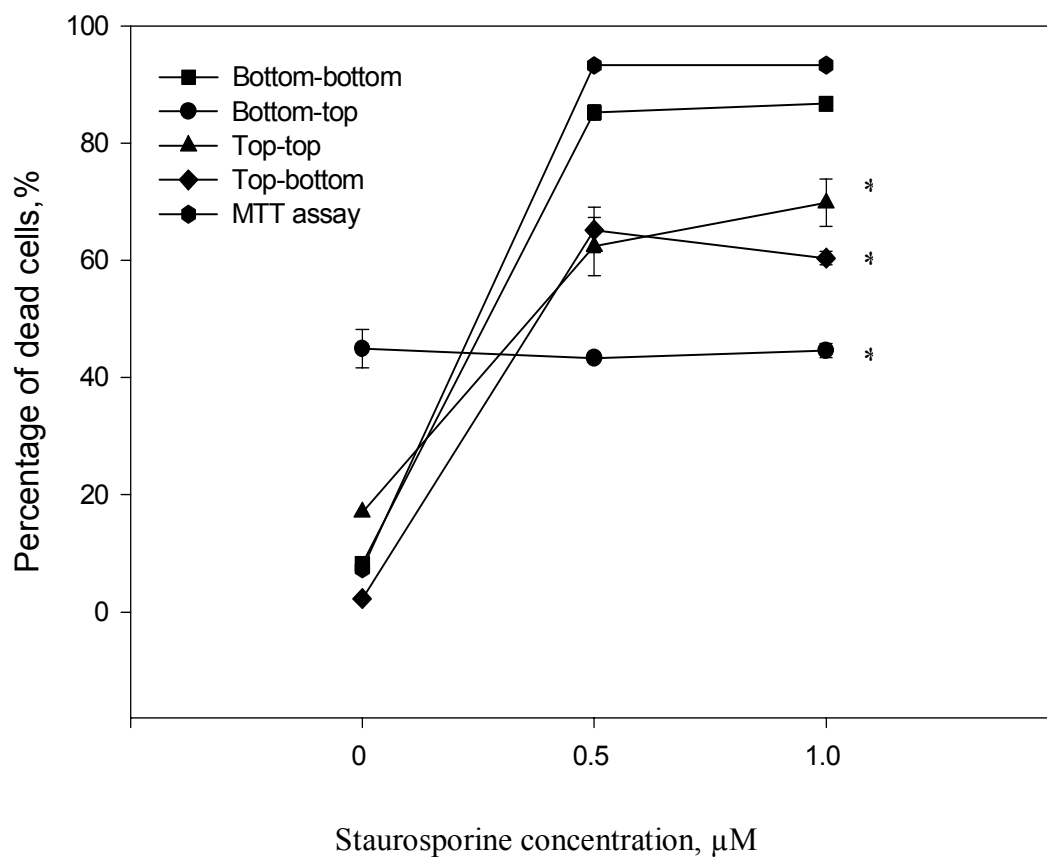


Figure 26. The percentage of dead cells after 20 hours of incubation with various concentrations of staurosporine. Untreated cells were used as negative control. The PI assay was conducted with four different optics settings of the microplate reader * statistically different from MTT assay results ($P < 0.05$).

The data in Figure 26 indicate a low percentage of dead cells in untreated samples and show a high percentage of cell death in cells treated with staurosporine. This shows that the assay worked well. It can be seen that the PI assay carried out with bottom-bottom optics gives results closest to those obtained with the MTT assay. In this research, those fluorescence readings were therefore done with bottom-bottom settings.

Dose and time-dependent viability of RAW 264.7 macrophages treated with TPGS

(a) Confluent (2×10^6 cells/well) RAW 264.7 cells were seeded in a 96-well plate and left overnight to attach to the bottom of the wells. They were then incubated with TPGS-enriched medium at concentrations of 12.4, 24.8, 37.2, and 49.6 μM for 24 hours. Cell viability was determined using the PI, CFDA and MTT assays as shown in Figures 27, 28, and 29, respectively.

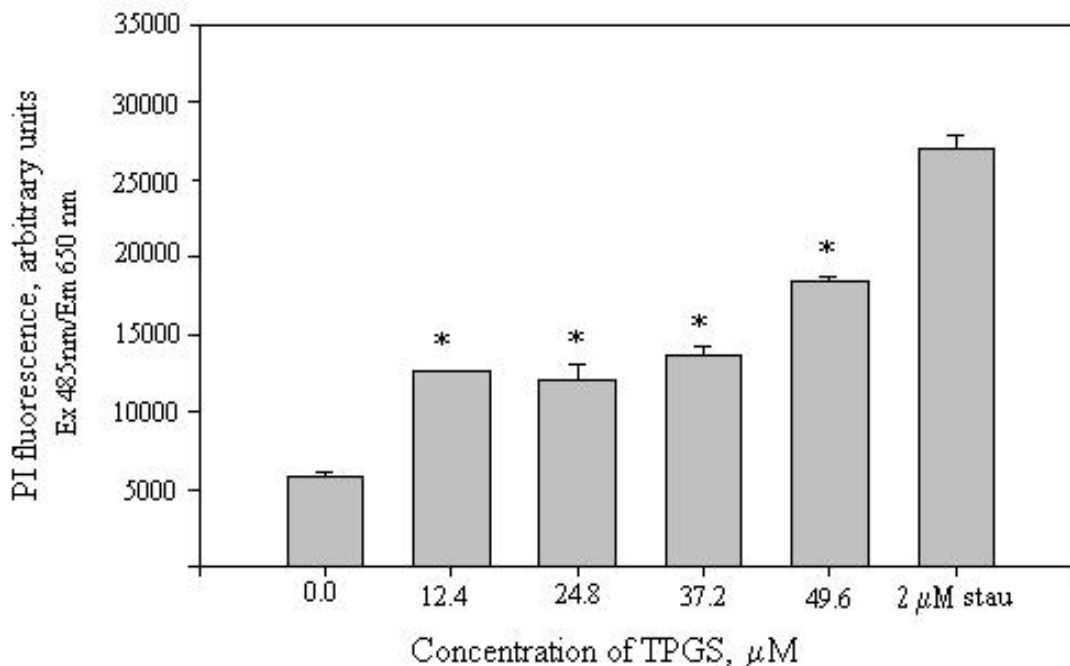


Figure 27. PI assay of RAW 264.7 macrophages viability after 24 hours of incubation with increasing concentrations of TPGS-enriched medium. Untreated cells and cells incubated with 2 μM staurosporine (stau) were used as negative and positive controls, respectively. * Statistically different from the negative control ($P \leq 0.05$). Values are means \pm S.E.M from 4 wells.

It can be observed from Figure 27 that a significant increase in the population of dead cells occurs when macrophages are exposed overnight to concentrations of TPGS at or greater than 12.4 μM . The high population of dead cells with the staurosporine positive control showed that this assay worked well.

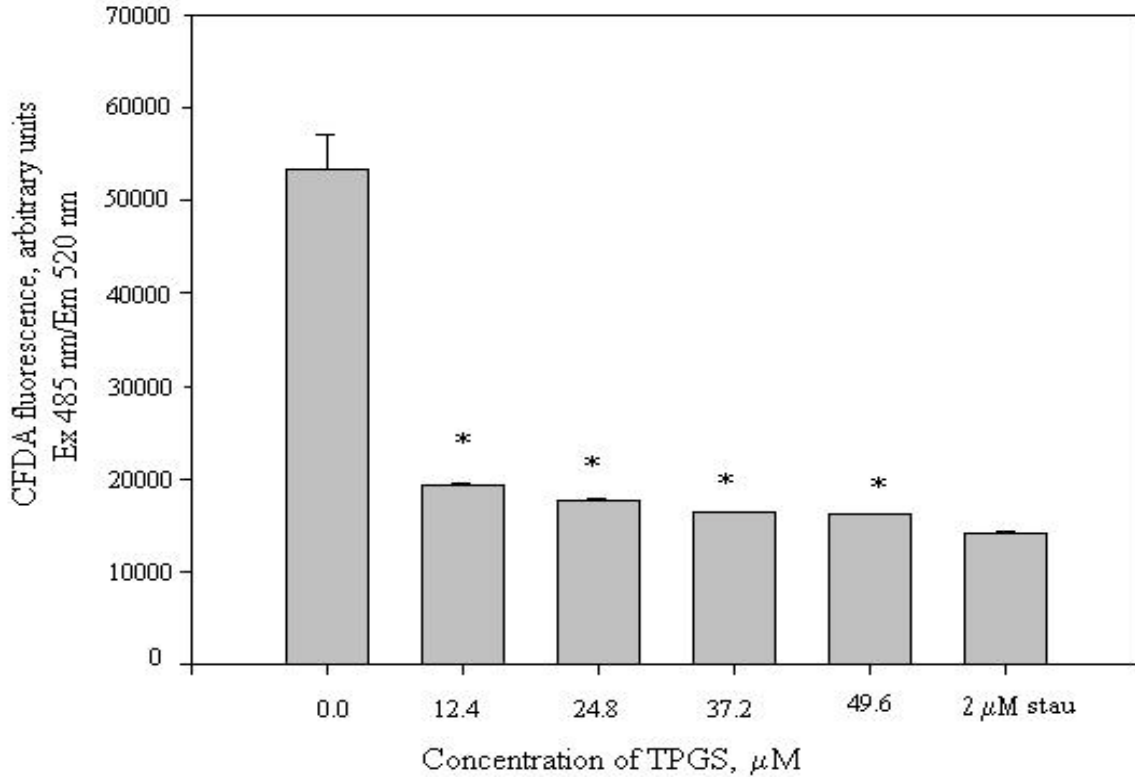


Figure 28. RAW 264.7 macrophages viability after 24 hours of incubation with TPGS, as measured by the CFDA assay. Untreated cells and cells incubated with 2 μM staurosporine (stau) were used as negative and positive controls, respectively. * Statistically different from the negative control ($P \leq 0.05$). Values are means \pm S.E.M from 4 wells.

It is observed from Figure 28 that the CFDA fluorescence signal produced by live cells is significantly reduced after treatment with TPGS concentrations equal to or greater than 12.4 μM . This indicates a decrease in the population of live cells. The low population of live cells with the staurosporine positive control confirmed the effectiveness of this assay.

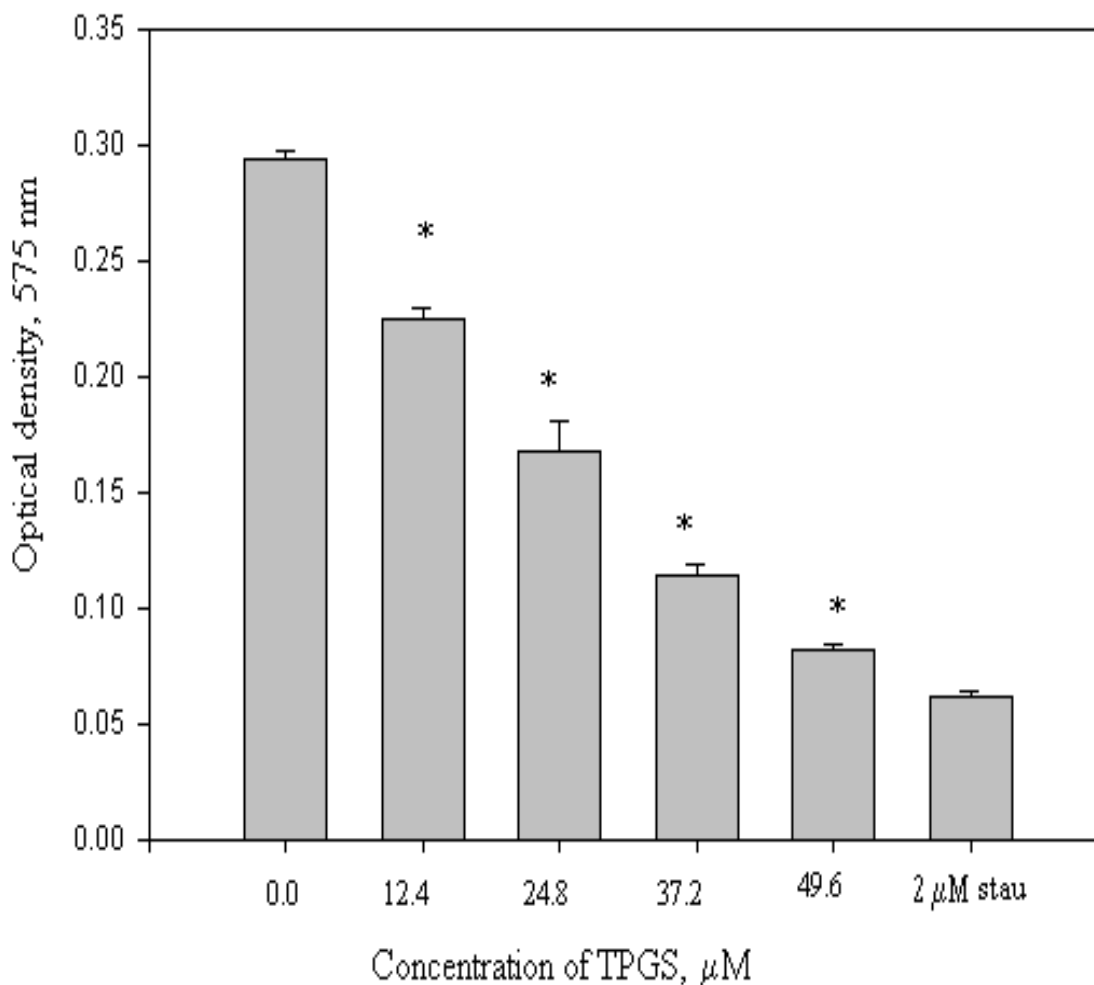


Figure 29. RAW 264.7 macrophages viability as measured with the MTT assay after 24 hours incubation with TPGS. Untreated cells and cells incubated with 2 μM staurosporine (stau) were used as negative and positive controls, respectively. * Statistically different from the negative control ($P \leq 0.05$). Values are means \pm S.E.M from 4 wells.

The decrease in mitochondrial activity observed in Figure 29 with increasing concentrations of TPGS confirms cell death is caused by TPGS concentrations $\geq 12.4 \mu\text{M}$ and is dose-responsive. The low population of live cells with the staurosporine positive control confirmed this assay worked well.

(b) To test for time-dependence, RAW 264.7 cells were seeded in a 96-well plate and left overnight to attach to the bottom of the wells and then incubated with 24.8 μM TPGS for 0, 4, 16, and 24 hour (s). Figure 30 shows results of cell viability as assessed with CFDA.

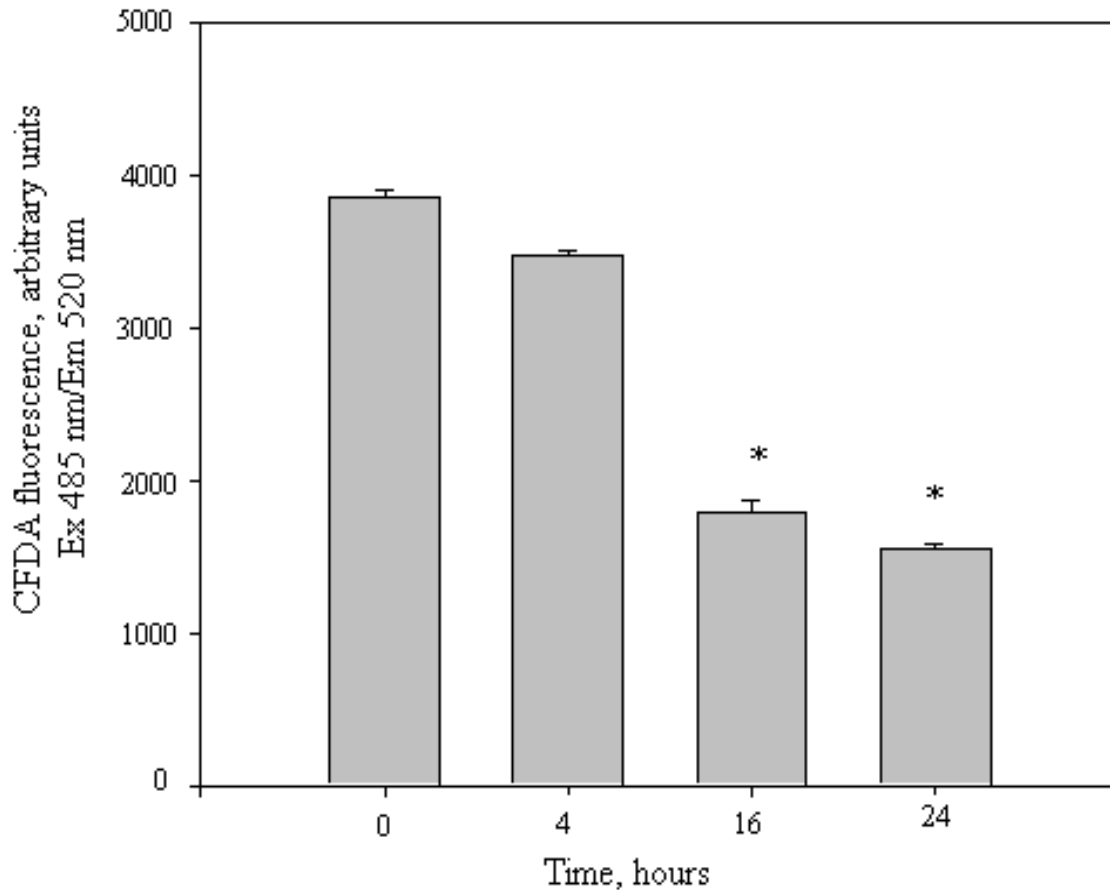


Figure 30. Time-dependent CFDA assay for RAW 264.7 macrophages viability after incubation with 24.8 μM TPGS. At time 0, TPGS was added to cells then withdrawn immediately. * Statistically different from 0 hour ($P \leq 0.05$). Values are means \pm S.E.M from 4 wells.

As shown in Figure 30, the population of live cells decreased with increasing time of incubation. Significant decreases were observed at 16 hours but not at 4 hours.

Comparative Viability of RAW 264.7 and LNCaP Cells Treated with TPGS

RAW 264.7 or LNCaP cells were seeded in 96-well plates and after an overnight incubation in medium, then they were treated with increasing concentrations of TPGS solutions for 24 hours. The number of live cells was assessed using the MTT assay. Figure 31 shows the changes observed in mitochondrial activity.

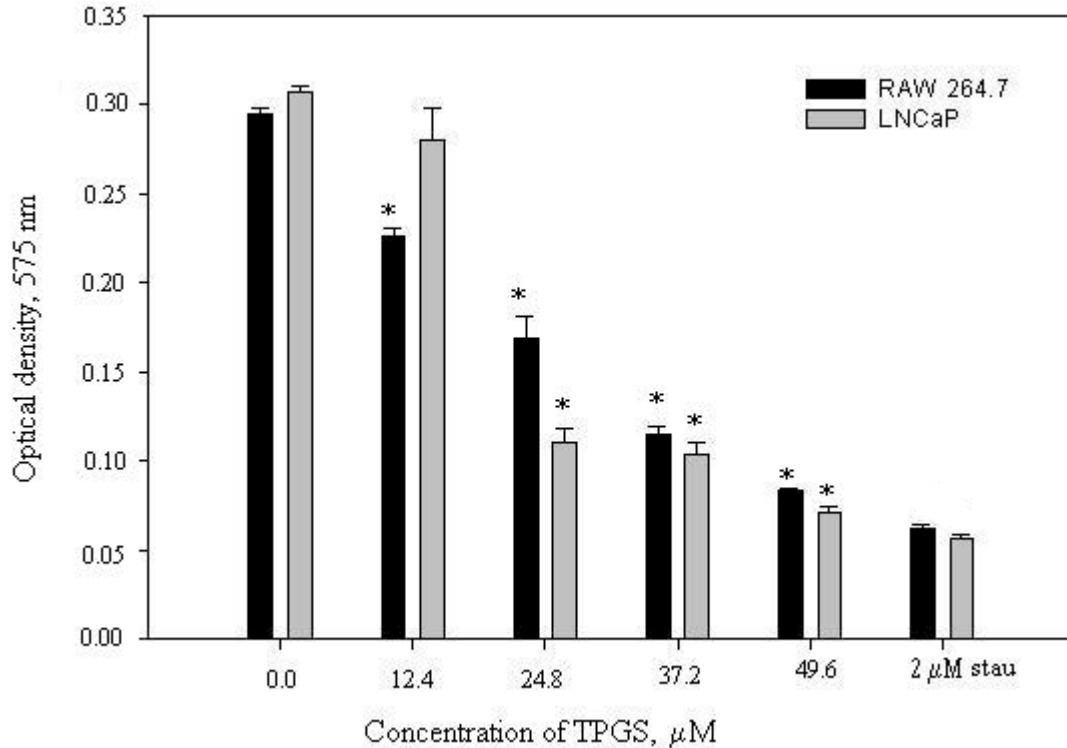


Figure 31. MTT assay of RAW 264.7 and LNCaP cells incubated with TPGS for 24 hours. Untreated cells and cells incubated with 2 μM staurosporine (stau) were used as negative and positive controls, respectively. * Statistically different from untreated cells ($P \leq 0.05$). Values are means \pm S.E.M from 4 wells.

It can be observed from Figure 31 that there is a decrease in mitochondrial activity with increasing concentrations of TPGS. This indicates that cell death is dose-dependent for both cell lines. However, a significant reduction in the number of live macrophages and LNCaP cells occurred after initial treatment with 12.4 and 24.8 μM

TPGS, respectively. The high number of cell death caused by staurosporine, the positive control, confirmed the reliability of this assay.

Comparative Viability of RAW 264.7 and LNCaP Cells Treated with α -TS

RAW 264.7 or LNCaP cells were seeded in 96-well plates and incubated overnight for the cells to adhere to the bottom of the well plates. They were then treated with increasing concentrations of α -TS-enriched medium for 24 hours. The medium was removed and the number of live cells assessed using the MTT assay. Figure 32 shows the changes observed in mitochondrial activity.

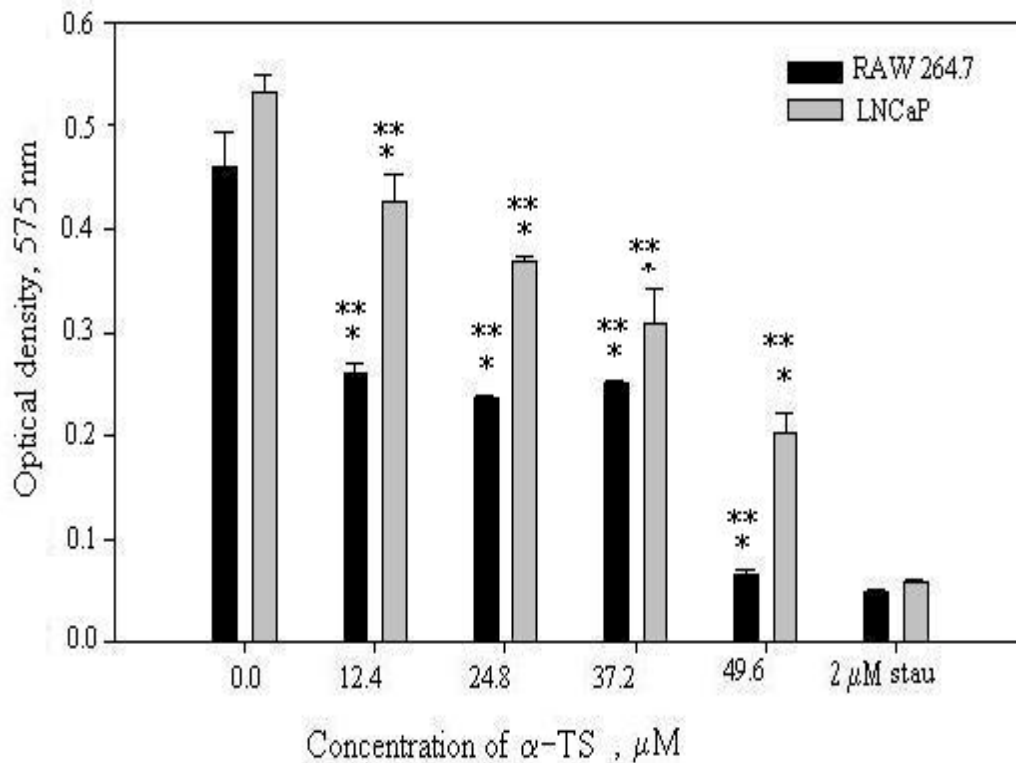


Figure 32. MTT assay of RAW 264.7 and LNCaP cells incubated with α -TS for 24 hours. * Statistically different from the other cell line, at the same concentration ($P \leq 0.05$). ** Statistically different from untreated cells ($P \leq 0.05$). Values are means \pm S.E.M from 4 wells.

In Figure 32, the reduction in mitochondrial activity observed with increasing concentrations of α -TS indicates that significant decrease in the number of live cells is dose-dependent for both cell lines and occurs after treatment with concentrations of α -TS $\geq 12.4 \mu\text{M}$. RAW 264.7 macrophages appear to be more sensitive than LNCaP cells when both are treated with the same concentration of α -TS. The low population of live cells with the staurosporine positive control this assay was successful.

Cellular Uptake of TPGS and α -TS

In order to identify the cause of cell death observed after incubation of RAW 264.7 and LNCaP cells with TPGS and α -TS, the cellular uptake and hydrolysis of these α -tocopheryl esters was measured using HPLC/ECD as described in the Methods Section. Cells were grown then seeded in 12-well plates. They were then incubated with TPGS or α -TS-enriched medium to allow the cellular uptake and hydrolysis. Lysis buffer was then added to break up the cell membranes and release any cellular tocopherol, which was then extracted in hexane and measured using HPLC/ECD. The uptake was measured as total tocopherol whereas free α -tocopherol indicates cellular hydrolysis of the esters. In these experiments, untreated cells were used as a control.

Dose-Dependent Uptake and Hydrolysis of TPGS and α -TS

RAW 264.7 or LNCaP cells were incubated with either TPGS or α -TS of concentrations 24.8 or 49.6 μM TPGS for 24 hours. The amounts of free and total tocopherol recovered from TPGS are shown in Figures 33 and 34, respectively.

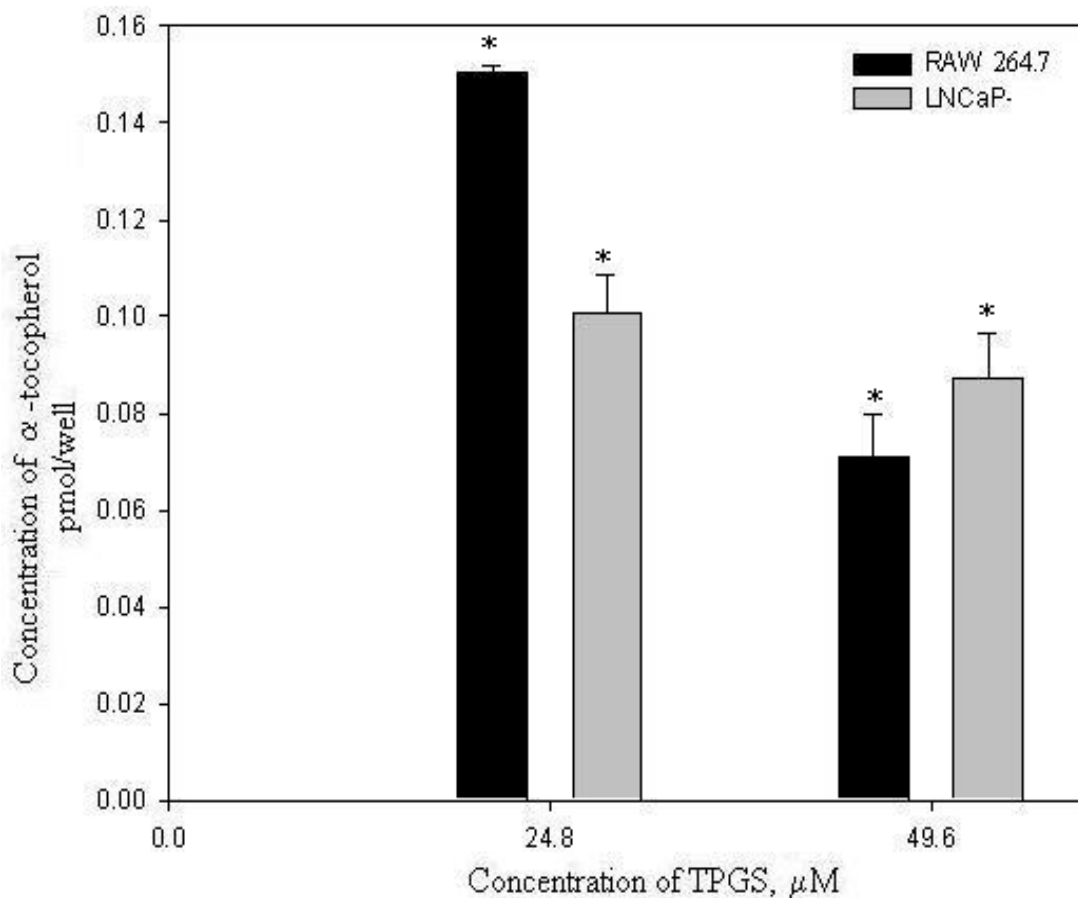


Figure 33. Cellular concentration of free tocopherol after 24 hours incubation with TPGS. Each well contained 1 mL of TPGS-enriched medium and after incubation, medium removal and cell washing, 1.5 mL of lysis buffer were added. α -Tocopherol from the cell lysate was then extracted into hexane and measured using HPLC/ECD. Lysate from untreated cells was used as control. Values are means \pm S.E.M from two experiments. * Statistical difference from the other cell line $P < 0.05$.

As shown in Figure 33, a significant difference was observed between the levels of free tocopherol from the hydrolysis of TPGS by RAW 264.7 macrophages and that by LNCaP cells.

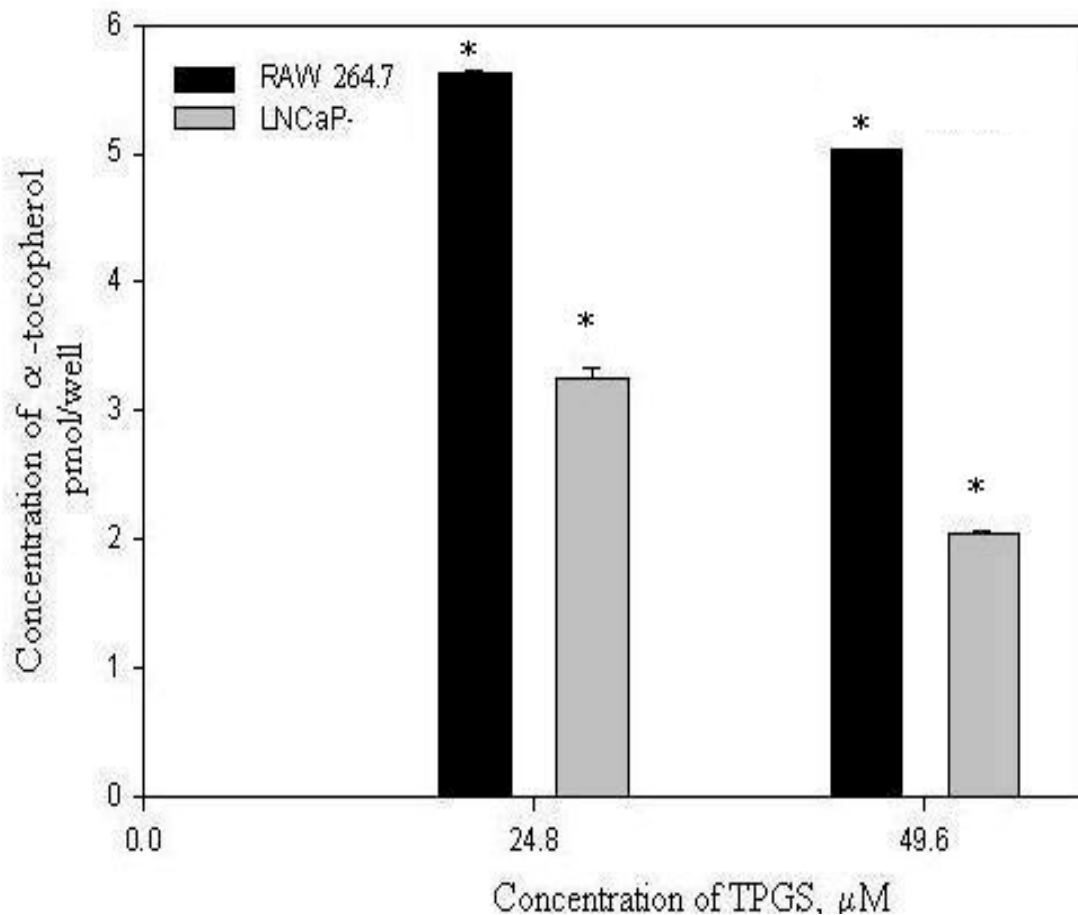


Figure 34. Cellular concentration of total tocopherol in RAW 264.7 and LNCaP cells after 24 hours incubation with TPGS. Each well contained 1 mL of TPGS-enriched medium and after incubation, medium removal and cell washing, 1.5 mL of lysis buffer were added. α -Tocopherol from the cell lysate was then extracted into hexane and measured using HPLC/ECD. Lysate prepared from untreated cells was used as control. Values are means \pm S.E.M from two experiments. * Statistically different from the other cell line, at the same TPGS concentration ($P \leq 0.05$).

The uptake of TPGS by RAW 264.7 macrophages was found to be greater than that observed for LNCaP cells (see Figure 34). The amounts of total tocopherol decreased with that of TPGS increasing because higher TPGS concentrations also cause more cell death.

The intracellular uptake (pmol/well) and hydrolysis of α -TS by RAW 264.7 and LNCaP cells, after a 24 hour incubation are shown in Figures 35 and 36, respectively.

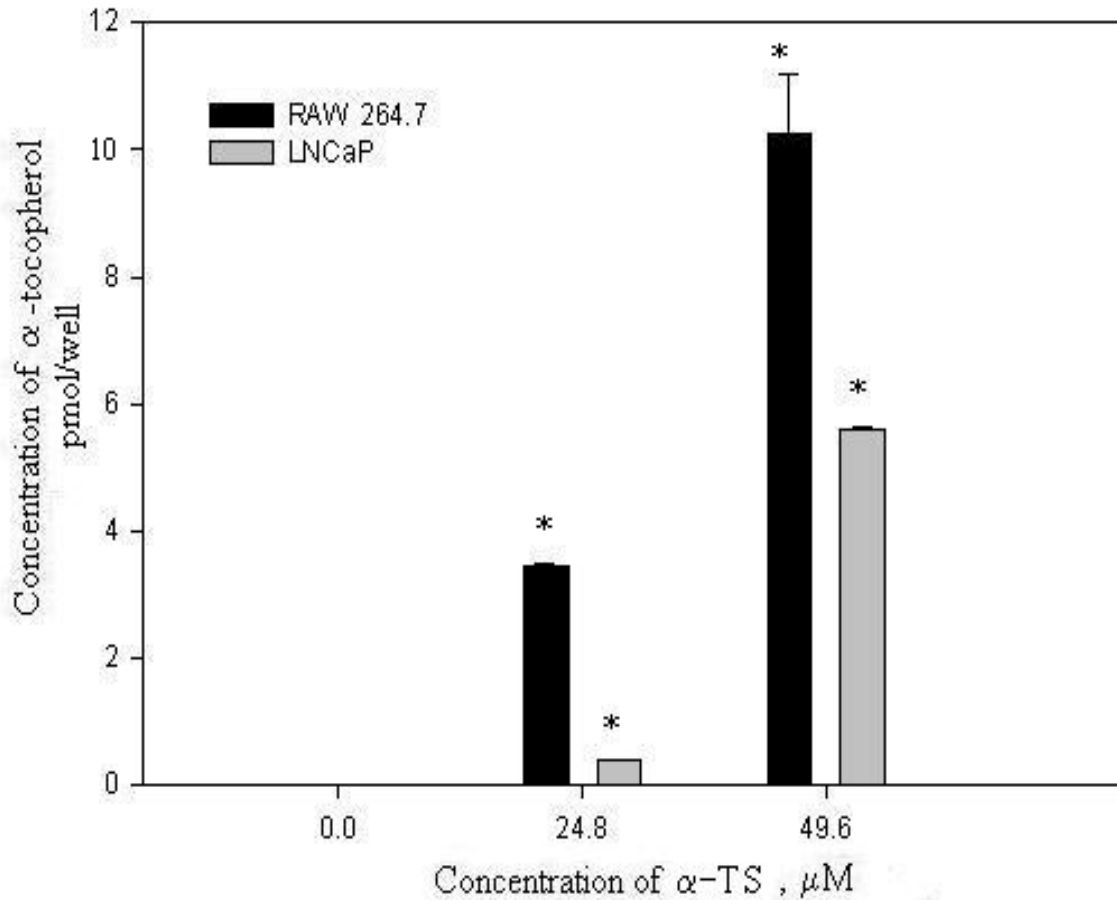


Figure 35. Cellular concentration of total tocopherol after 24 hours of incubation with α -TS. Each well contained 1 mL of α -TS-enriched medium. After the incubation, the medium was removed, the cells washed and 1.5 mL of lysis buffer were added. α -Tocopherol from the cell lysate was extracted into hexane and measured using HPLC/ECD. Values are means \pm S.E.M from two experiments. * Statistically different from the other cell line, at the same α -TS concentration ($P \leq 0.05$).

As shown in Figure 35, the cellular total tocopherol was shown to increase with increasing concentration of α -TS. RAW 264.7 macrophages took up significantly greater amounts of α -TS than LNCaP cells.

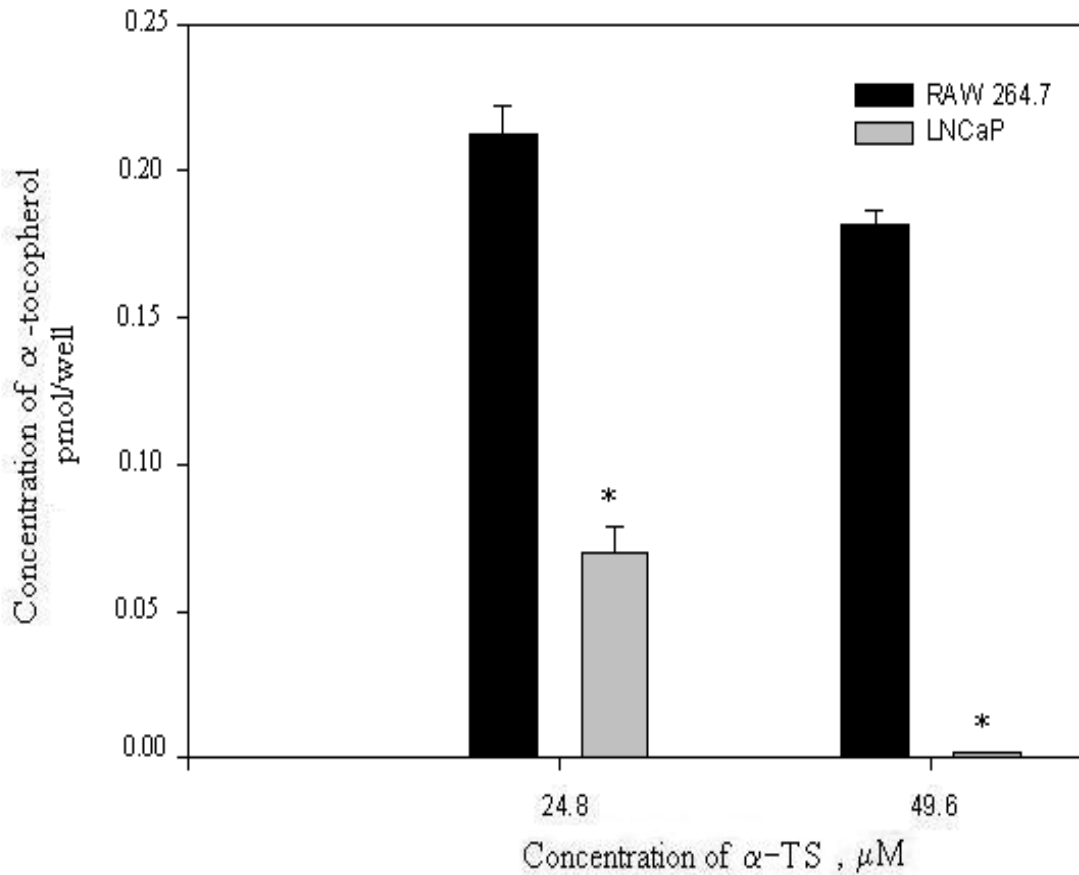


Figure 36. Cellular concentration of free tocopherol after 24 hours incubation with α -TS. After 24 hours of incubation with α -TS, the medium was removed, the cells washed, and 1.5 mL of lysis buffer were added per well. Cellular α -tocopherol was then extracted into hexane and measured using HPLC/ECD. Values are means \pm S.E.M from two experiments. * Statistically different from the other cell line, at the same α -TS concentration ($P \leq 0.05$).

As shown in Figure 36, the levels of free tocopherol decreased with increasing concentrations of α -TS. RAW 264.7 macrophages took up significantly greater amounts of α -TS than did LNCaP cells.

Table 3. Percentages of cellular tocopherol recovered in dose-dependent experiments. RAW 264.7 macrophages and LNCaP cells were incubated for 24 hours with 24.8 and 49.6 μM TPGS and $\alpha\text{-TS}$. Values are means \pm S.E.M from two experiments.

		TPGS, μM		$\alpha\text{-TS}$, μM	
		24.8	49.6	24.8	49.6
RAW 264.7 macrophages	Esterified tocopherol, % TPGS and/or $\alpha\text{-TS}$	97.3	98.7	93.9	98.2
	Free $\alpha\text{-TOH}$, %	2.7	1.3	6.1	1.8
LNCaP cells	Esterified tocopherol, % TPGS and/or $\alpha\text{-TS}$	96.9	95.7	82.4	100
	Free $\alpha\text{-TOH}$, %	3.1	4.3	17.6	0.0

Table 3 shows that the percentages of free tocopherol from intracellular hydrolysis of TPGS and $\alpha\text{-TS}$ are very small compared to the levels of TPGS and/or $\alpha\text{-TS}$. It can be also observed that, whereas the percentages of esterified tocopherol significantly increase with the concentration of $\alpha\text{-TS}$, the reverse is obtained for free tocopherol. The percentages of tocopherol from TPGS did not appear to follow any pattern. The data in Table 4, below, indicate that only a small amount of tocopherol is taken up by cells (intracellular). Most of the TPGS or $\alpha\text{-TS}$ added per well remains in the culture medium.

Table 4. Concentrations of intracellular and extracellular tocopherol in pmol/well.

	Tocopherol, Pmol/well	TPGS, pmol/well		α -TS, pmol/well	
		24800	49600	24800	49600
RAW 264.7 macrophages	Intracellular	5.63	5.36	3.45	10.26
	Extracellular	24794.37	49594.64	24796.55	49589.74
LNCaP cells	Intracellular	3.3	2.04	0.39	5.59
	Extracellular	24796.7	49597.96	24799.61	49594.41

Time-dependent uptake and hydrolysis of TPGS

RAW 264.7 and LNCaP cells were incubated with 24.8 μ M TPGS for 24, 48, and 72 hours.

Table 5. Percentages of cellular tocopherol recovered in time-dependent experiments. RAW 264.7 macrophages and LNCaP cells were incubated with 24.8 μ M TPGS for 24, 48, and 72 hours. Values are indicated as \pm S.E.M from two experiments.

	Time, hours	TPGS		
		24	48	72
RAW 264.7 macrophages	Esterified tocopherol, % TPGS/ α -TS	97.3	97.0	95.7
	Free α -TOH, %	2.7	3.0	4.3
LNCaP cells	Esterified tocopherol, % TPGS/ α -TS	96.9	97.1	96.9
	Free α -TOH, %	3.1	2.9	3.1

The data in Table 5 show that, unlike LNCaP cells, RAW 264.7 macrophages take up and hydrolyze TPGS in a time-responsive manner. This is most likely because macrophages contain higher levels of esterases.

Concentration Calibration Curves of α -TOH and 5, 7-DMT

In order to establish a relationship between optical density and concentration of standard solutions, six solutions of α -TOH and 5, 7 –DMT were prepared in ethanol and their absorbance measured using a Cary 50 Bio UV-Visible spectrophotometer. A scan was performed with baseline correction from 200 nm to 350 nm. The maximum absorbance at 292 nm was recorded. Beer's law and molar extinction coefficients ($\epsilon = 3460$ and $3270 \text{ cm}^{-1}\text{M}^{-1}$ for 5, 7-DMT and α -TOH, respectively) were then used to calculate concentrations according to the formula:

$$C = OD / (\epsilon_{\lambda} \times l)$$

C = Concentration in M

OD = Optical density

ϵ = Molar extinction coefficient, $\text{cm}^{-1}\text{M}^{-1}$

l = Pathlength of measuring light beam.

[A]= stock solution; [B] = [A]/2; [C] = [A]/4; [D] = [A]/8; [E] = [A]/16; [F] = [A]/32.
Beer's law and molar extinction coefficients were then used to calculate concentrations.
For example, 5, 7-DMT has $\epsilon_{\lambda} = 3460 \text{ cm}^{-1}\text{M}^{-1}$ at 292 nm.

$$\text{Solution A: } [A] = 0.75/3460 = 216.18 \text{ } \mu\text{M}$$

$$\text{Solution B: } [A]/2 = 0.37/3460 = 213.29 \text{ } \mu\text{M}$$

The average of these two values was calculated as [A],

$$[A] = (216.18 \text{ } \mu\text{M} + 213.29 \text{ } \mu\text{M})/2 = 215.04 \text{ } \mu\text{M}$$

Concentrations of solutions B, C, D, E and F were then obtained from [A]:

$$[B] = 107.52 \text{ } \mu\text{M} \quad [C] = 53.76 \text{ } \mu\text{M} \quad [D] = 26.88 \text{ } \mu\text{M} \quad [E] = 13.44 \text{ } \mu\text{M} \quad [F] = 6.72 \text{ } \mu\text{M}$$

Concentrations of standard α -TOH solutions were calculated the same way using the molar extinction coefficient of $3270 \text{ cm}^{-1}\text{M}^{-1}$ at 292 nm.

[A]= 301.69 μM [B] = 150.84 μM [C] = 75.42 μM [D] = 37.71 μM
[E] = 18.86 μM [F] = 9.43 μM

Linear curves of optical density versus concentration were then plotted as shown in Figures 37 and 38 and the linear relationship obtained.

5,7-DMT: Optical density = 0.0035 (concentration) - 0.0038

α -TOH: Optical density = .0032 (concentration) + 0.0082

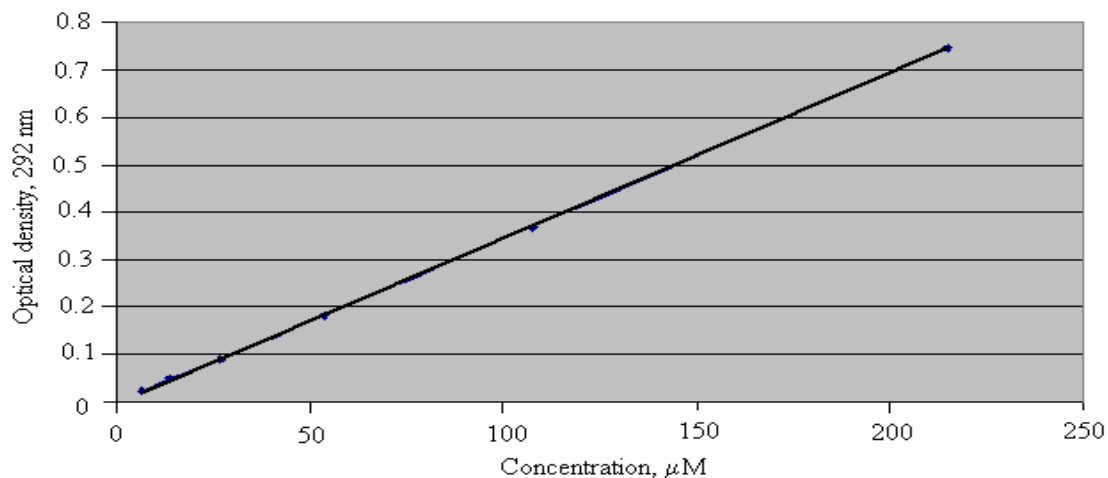


Figure 37. Linear relationship between optical density and concentration for 5, 7-DMT.

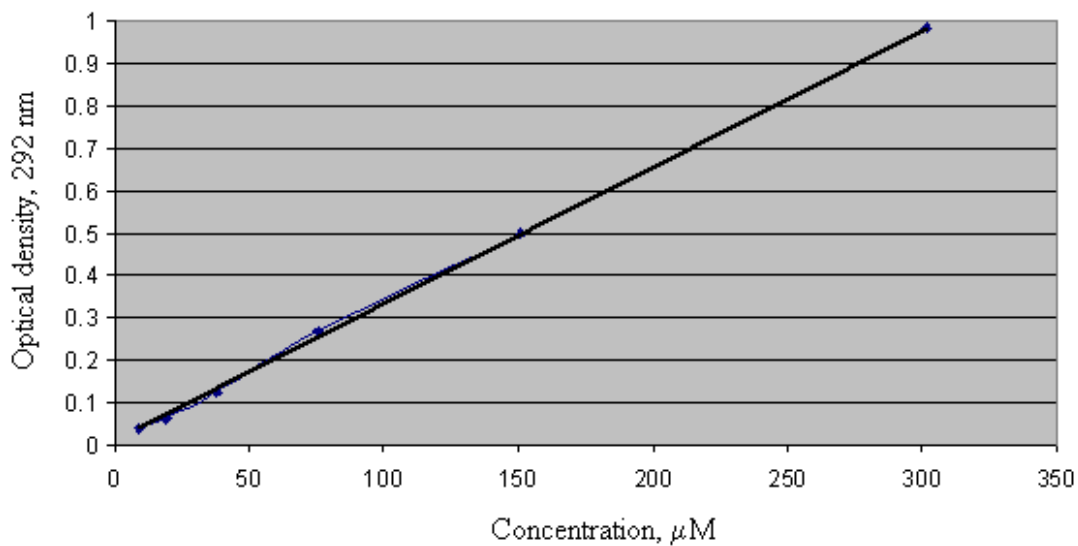


Figure 38. Linear relationship between optical density and concentration for α -TOH

Properties of p-HATS

Oxidation Potential for Electrochemical Detection of p-HATS.

p-HATS possess a free hydroxyl group and is therefore electroactive. In order to determine its chromatographic properties, the optimum oxidation potential for its detection using HPLC/ECD was found. A mixture of 250 pmol *p*-HATS and 79 pmol of 5, 7-DMT was prepared in mobile phase and the peaks recorded at different oxidation potentials. Figure 39 shows the *p*-HATS peak areas obtained as a function of the oxidation potential used.

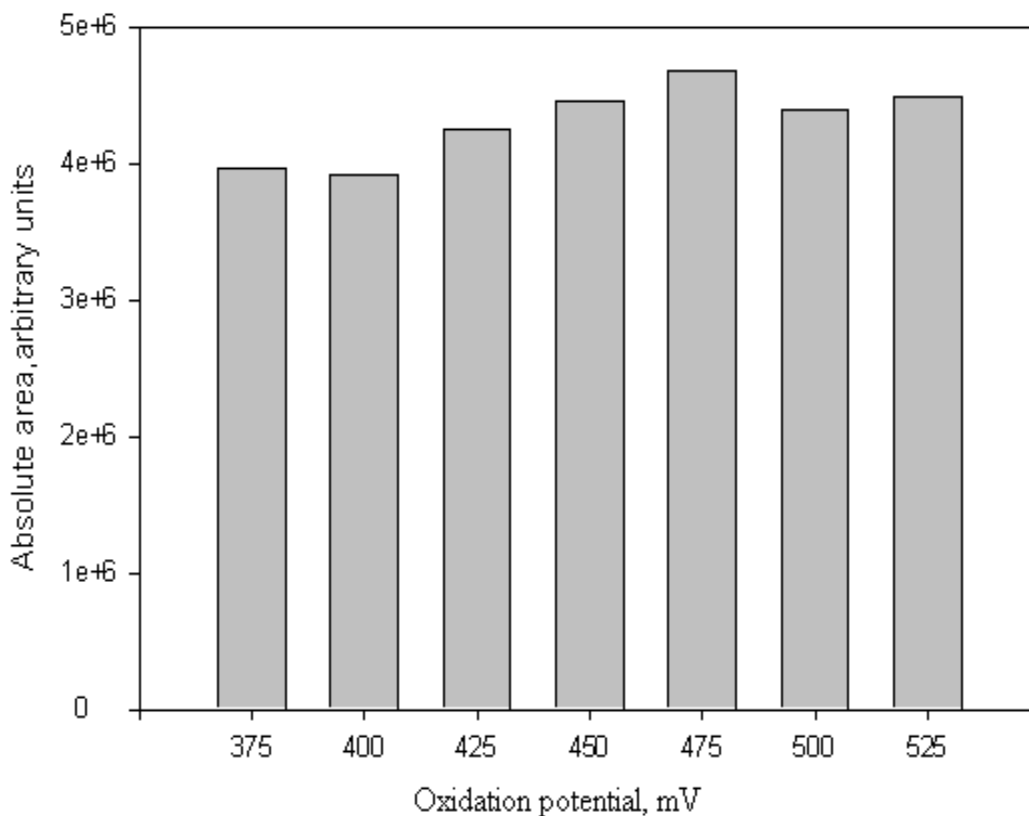


Figure 39. Absolute peak areas of *p*-HATS as a function of oxidation potential. A solution of *p*-HATS and 5, 7-DMT was prepared in mobile phase and the two compounds detected using HPLC/ECD.

The data in Figure 39 show that no significant differences were found in the absolute areas of *p*-HATS as the oxidation potential was varied. Therefore, 400 mV, the potential used in previous experiments for the detection of α -TOH was used to analyze *p*-HATS because this potential is optimal for vitamin E.

Retention Time of *p*-HATS Relative to 5, 7-DMT.

A solution of 417 pmol *p*-HATS, 2.30 pmol 5, 7-DMT and 2.42 pmol α -TOH was prepared in mobile phase and injected into the HPLC for analysis. Figure 40 shows the chromatogram obtained from this measurement.

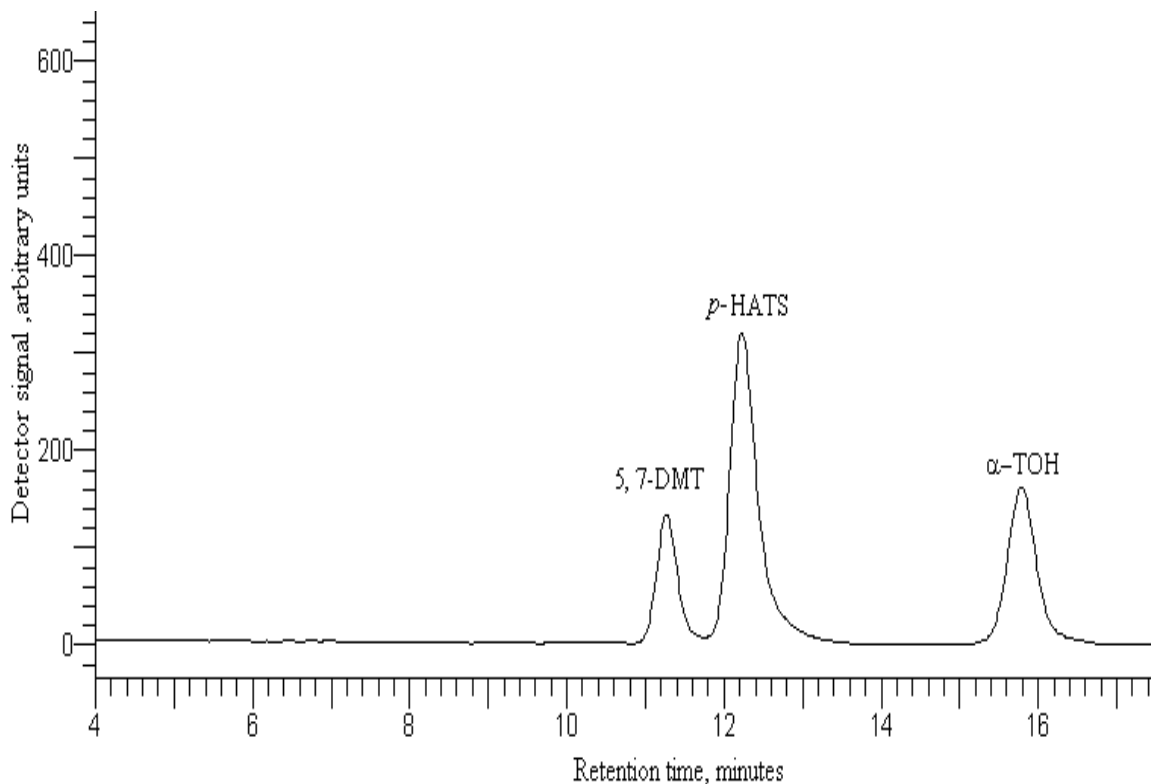


Figure 40. Chromatogram of a mixture of *p*-HATS and 5, 7-DMT in mobile phase.

It can be seen from Figure 40 that *p*-HATS is indeed electroactive and elutes from the column later than 5, 7-DMT and earlier than α -TOH. The absence of extra peaks suggests that the by-product of *p*-HATS synthesis, *p*-HA, was not present as an impurity in the sample.

Retention Time of *p*-HA Relative to 5, 7-DMT.

In order to confirm that *p*-HA eluted at a retention time different from that of 5, 7-DMT and *p*-HATS, a solution of 120 pmol *p*-HA and 55 pmol 5, 7-DMT in mobile phase was prepared and analyzed using HPLC/ECD. The peaks obtained are shown in Figure 41.

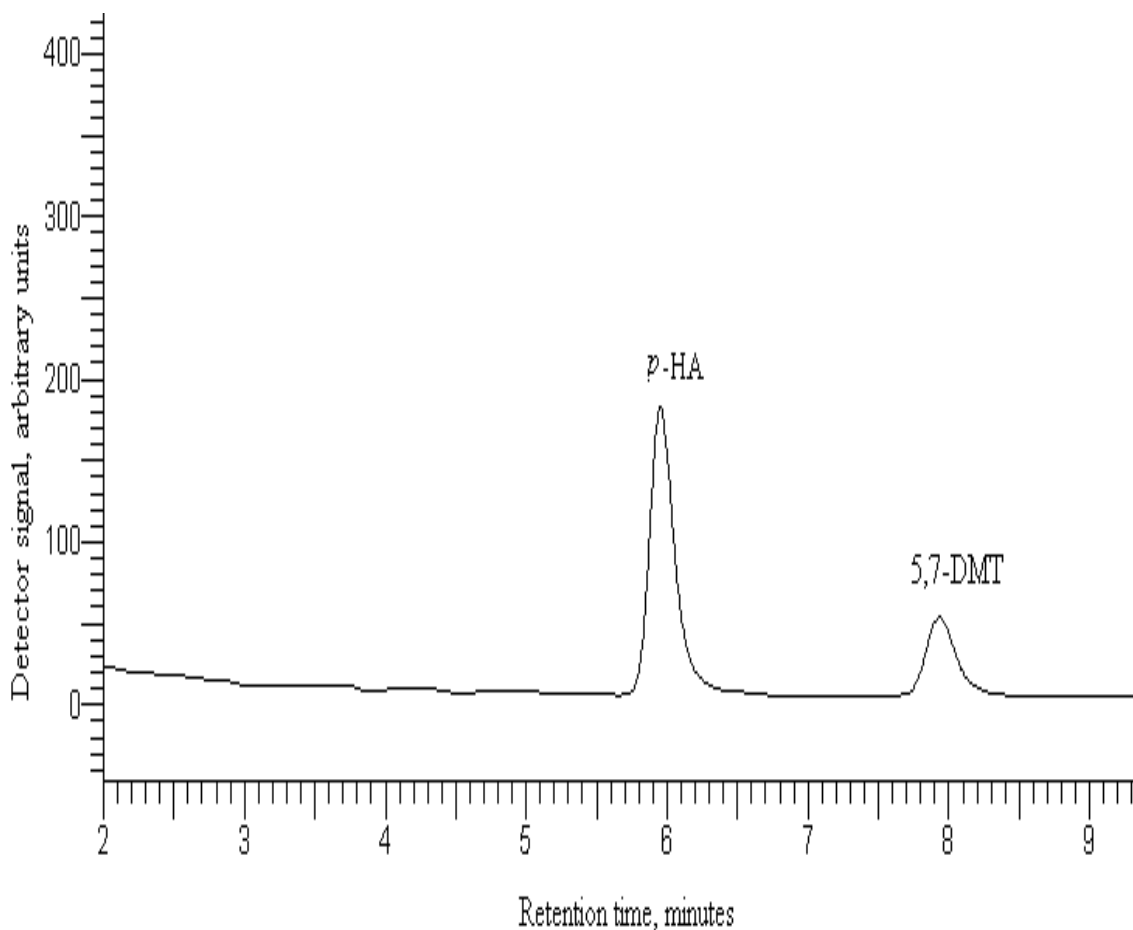


Figure 41. Chromatogram of a solution of *p*-HA and 5, 7-DMT in mobile phase.

The chromatogram in Figure 41 shows that *p*-HA elutes from the non-polar chromatographic column earlier than 5, 7-DMT. The position of this peak also proves the *p*-HATS synthesized was free of this by-product.

Extraction of *p*-HATS.

The extraction of α -TOH was carried out in hexane throughout this study. It was therefore assumed that hexane might also be a suitable solvent for *p*-HATS. A solution of 25 μ M *p*-HATS was prepared, treated with antioxidants as described earlier in the Methods Section, and extracted into hexane. Figures 42 and 43 show the chromatograms obtained in the mobile phase and after extraction into hexane, respectively.

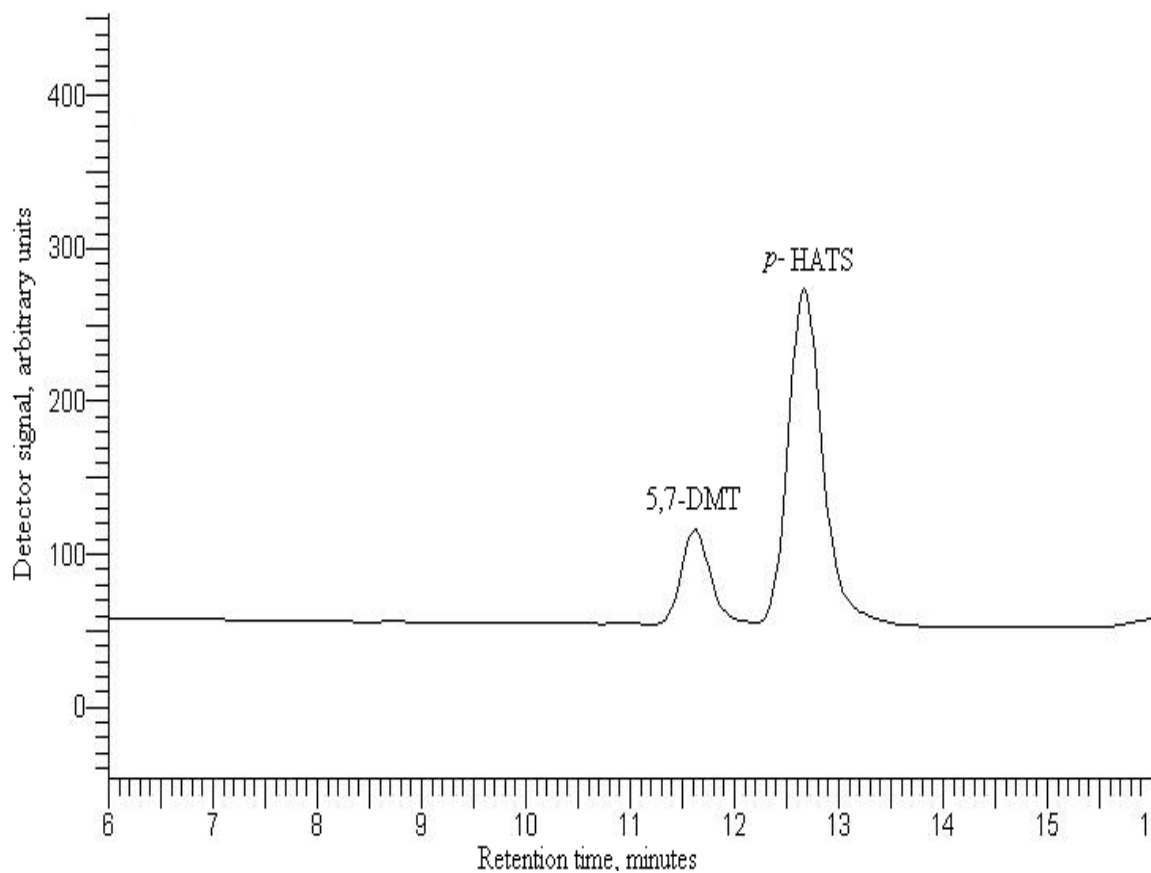


Figure 42. Detector signal as a function of retention time for a solution of 750 pmol *p*-HATS and 288 pmol 5, 7-DMT in mobile phase.

The areas under the peaks in Figure 42 were obtained and used to calculate the response factor. *F* was found to be 0.6194 ± 0.0052 .

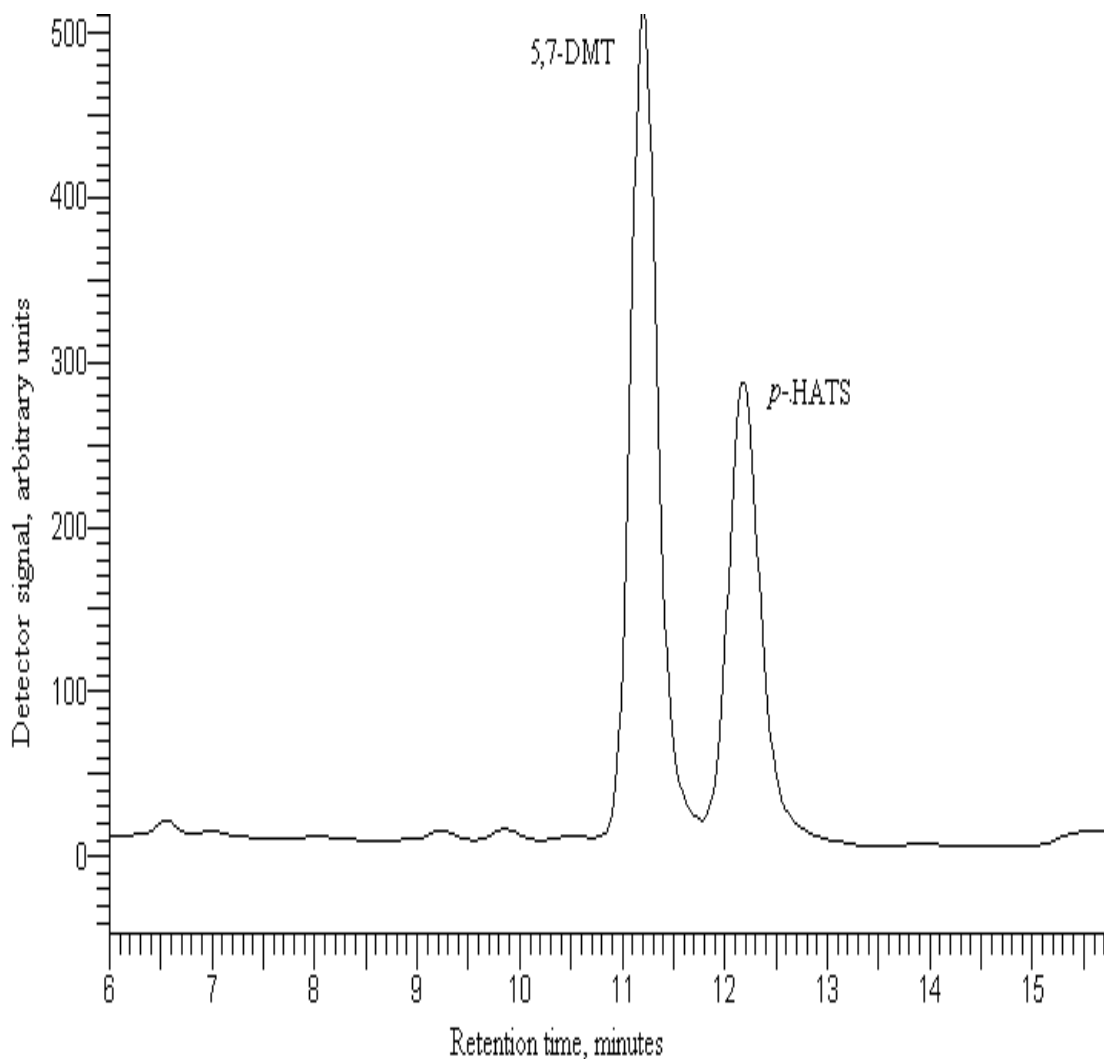


Figure 43. Chromatogram of a solution of *p*-HATS extracted into hexane.

The response factor ($F=4.4906$) calculated from the areas under the peaks in Figure 43 was significantly different from that obtained in Figure 42. Much less *p*-HATS was recovered for the condition in Figure 43 than in Figure 42. This suggested that hexane is not suitable for the extraction of *p*-HATS. Other solvents were therefore considered.

The chromatograms obtained after extraction of 12.5 nmol of *p*-HATS into octane, methylene chloride, and ethyl acetate are shown in Figures 44, 45, and 46, respectively.

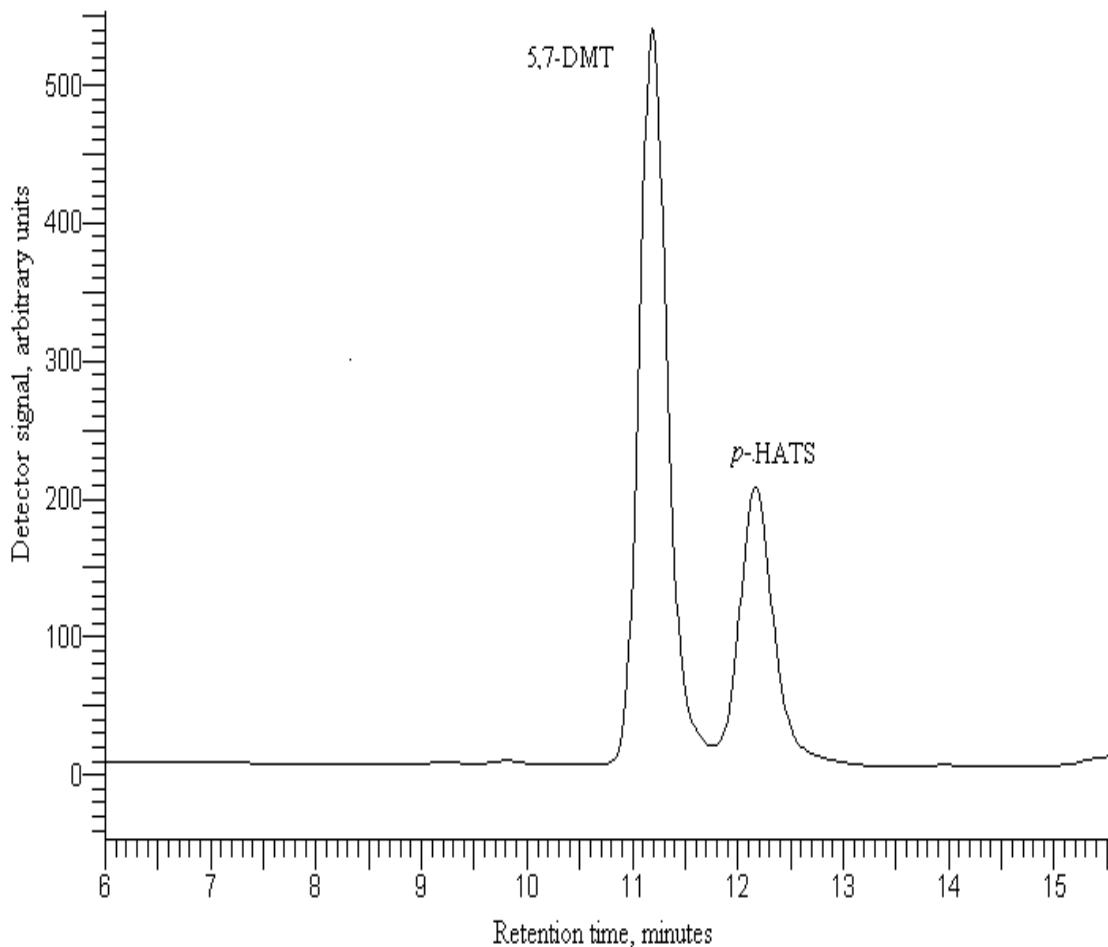


Figure 44. Chromatogram of a solution of *p*-HATS extracted into octane.

Figure 44 shows that low levels of *p*-HATS were obtained after an extraction using octane. The response factor ($F = 5.755$) obtained was very high relative to that in Figure 42. Octane, as well as hexane, are straight hydrocarbon chains and have a polarity index of 0.00. The amide group in *p*-HATS makes the compound very polar compared to TPGS. This is the reason why methylene chloride and ethyl acetate were also evaluated.

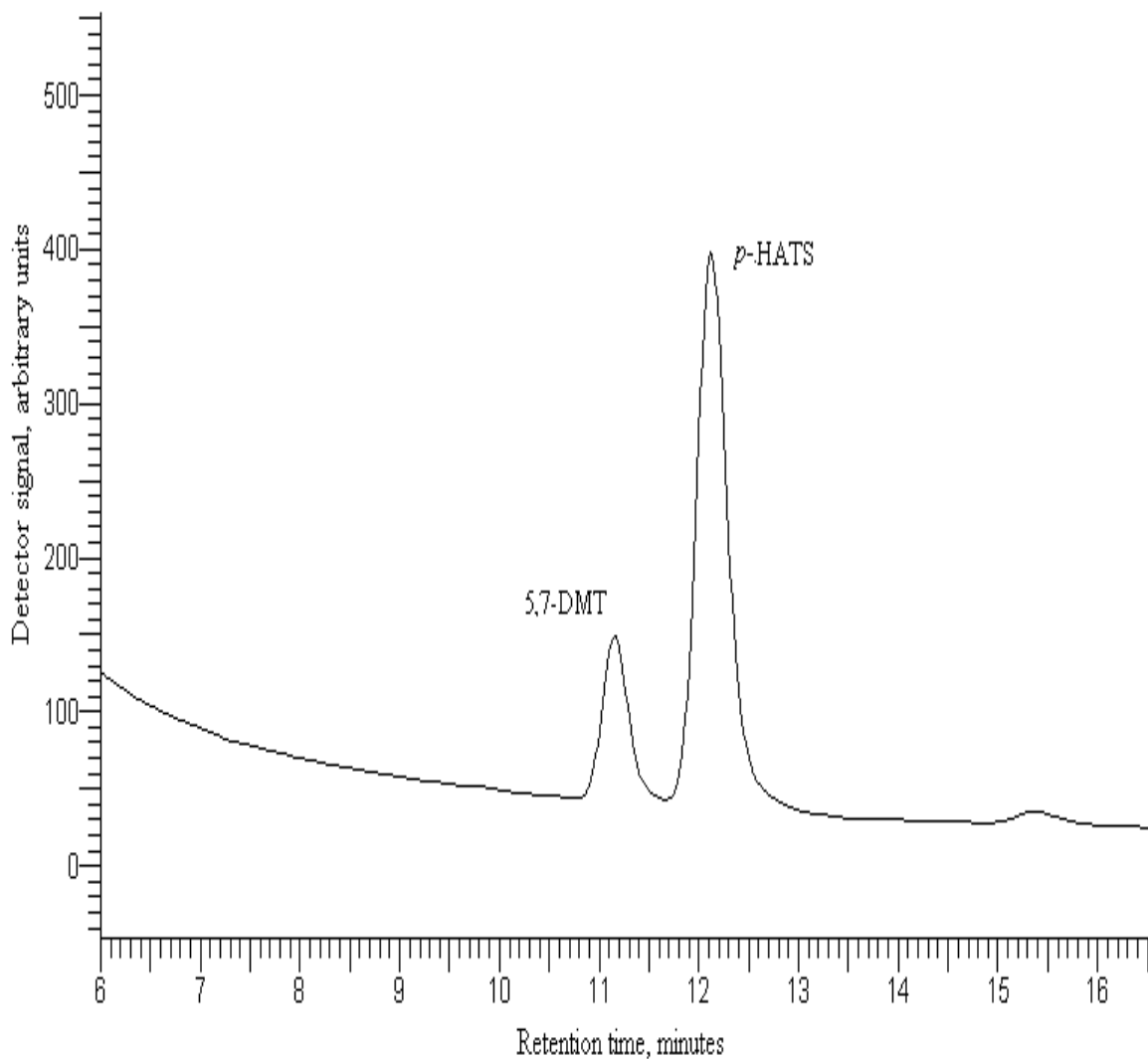


Figure 45. Chromatogram of a solution of *p*-HATS extracted into methylene chloride.

When methylene chloride was used as extracting solvent, high levels of *p*-HATS were recovered. Indeed, this solvent has a polarity index of 3.1 and was shown to solubilize *p*-HATS better than hexane or octane. However, it took more than an hour to dry 500 μL of the methylene chloride under nitrogen. The response factor obtained, 0.6489, was close to the value calculated from Figure 42.

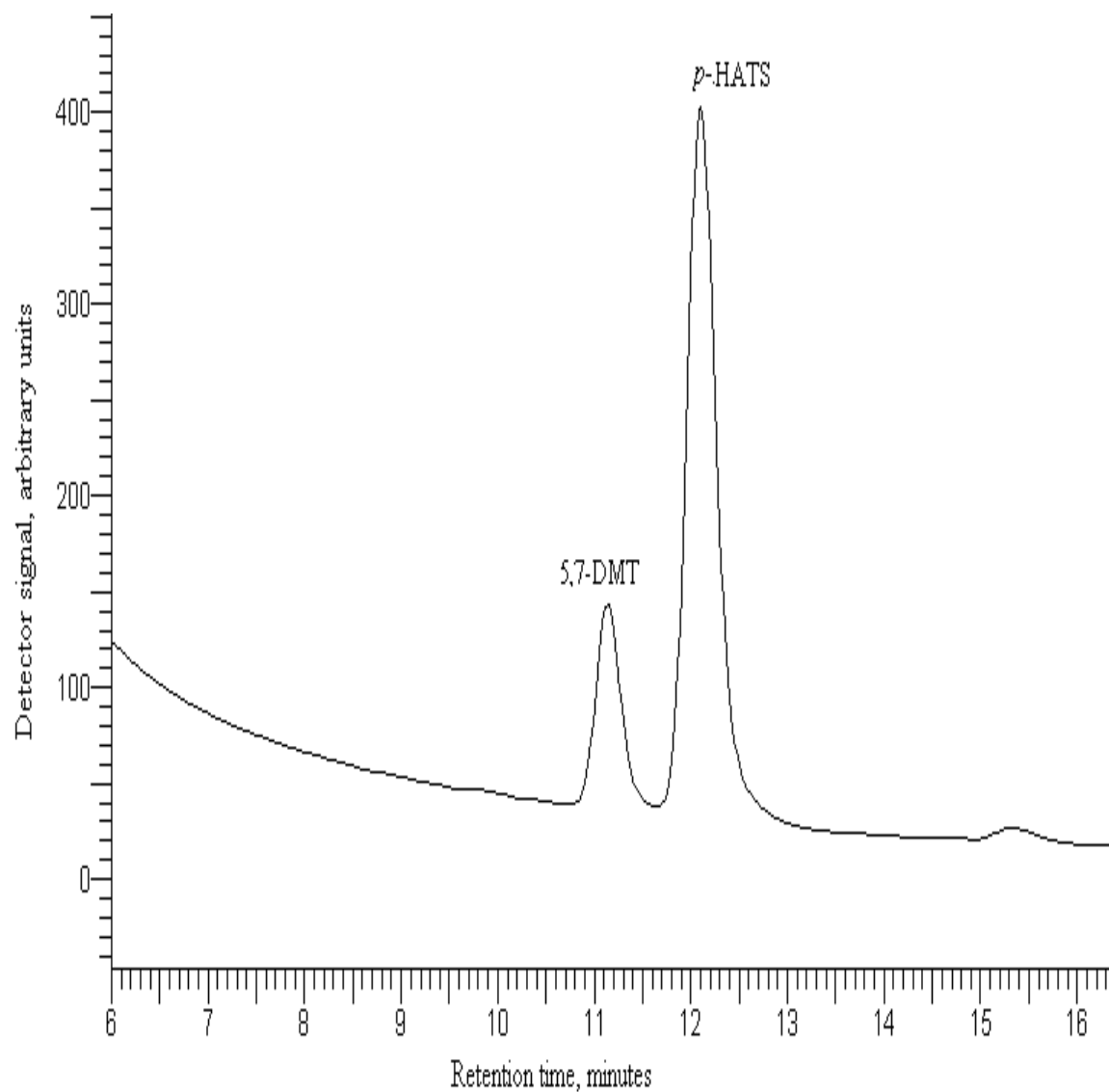


Figure 46. Chromatogram of a solution of *p*-HATS extracted into ethyl acetate.

As shown in Figure 46, ethyl acetate also extracted high levels of *p*-HATS. From all the solvents used, it gave a response factor ($F = 0.6355$) closest to the value obtained in mobile phase. It took only 30 minutes to dry 500 μL of the ethyl acetate layer under nitrogen. Therefore, compared to methylene chloride, it would be a better solvent for the extraction of *p*-HATS.

Hydrolysis of *p*-HATS.

A 25 μM solution of *p*-HATS was prepared in ethanol; a 500 μL aliquot was then treated with antioxidants and saponified with 300 μL of saturated KOH for 5 minutes. The products of *p*-HATS hydrolysis were then extracted into ethyl acetate and hexane and analyzed using HPLC/ECD. Figures 47 and 48 show the peaks obtained with ethyl acetate and hexane, respectively.

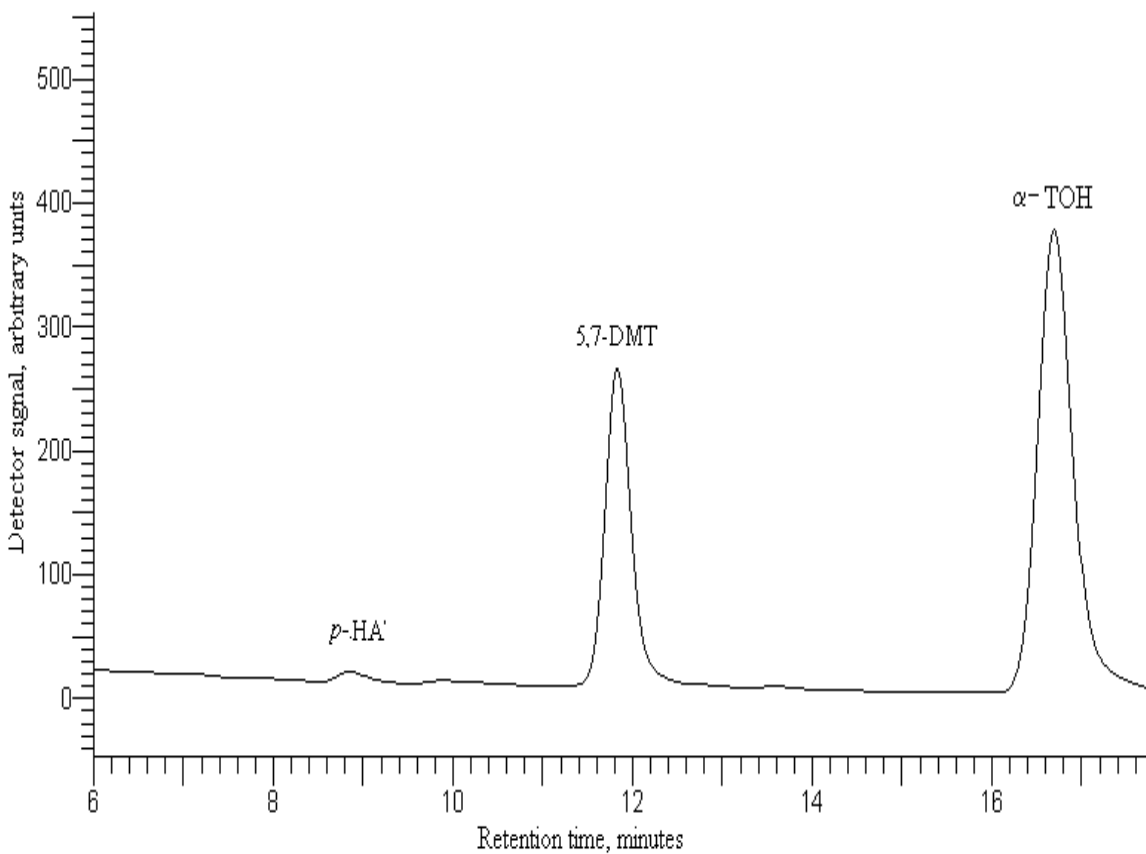


Figure 47. Chromatogram of a saponified solution of *p*-HATS after extraction into ethyl acetate.

It can be seen from Figure 47 that, in addition to the internal standard peak, two compounds elute at times 8.9 and 16.6 minutes. In Figure 41, *p*-HA eluted approximately 2 minutes before 5, 7-DMT. The chromatogram in Figure 40 showed that α-TOH elutes

about 4 minutes 5, 7-DMT. These facts suggest that *p*-HA and α -TOH might be hydrolysis products of *p*-HATS .

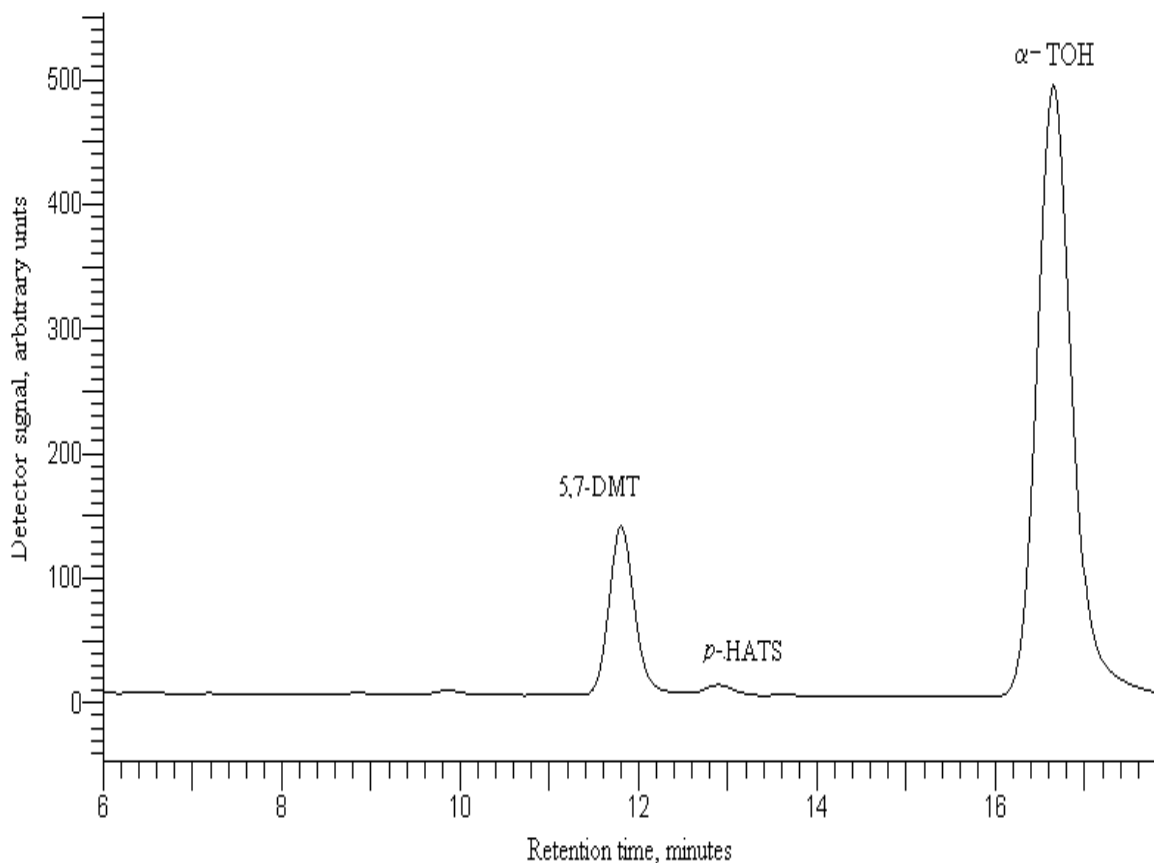


Figure 48. Chromatogram of a saponified solution of *p*-HATS after extraction into hexane.

From figure 48, it can be observed that a low amount of *p*-HA eluted after 10 minutes. This confirms the fact that it is one of the hydrolysis products of *p*-HATS. It should also be noted that the peak at 16.6 minutes is strong in both Figures 47 and 48, when ethyl acetate and hexane are used, respectively. Therefore, the extracting solvent used did not affect the recovery of the product(s). These results also suggest that the compound is probably α -TOH.

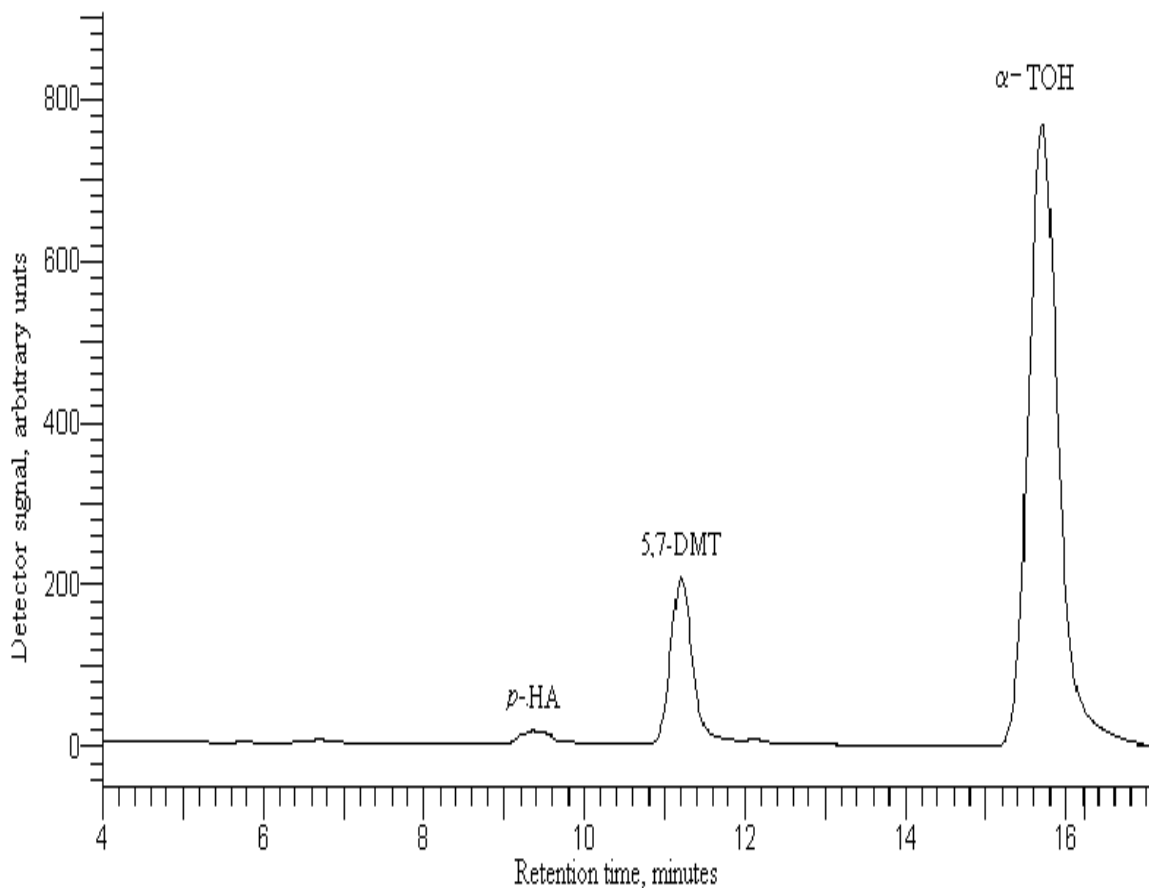


Figure 49. Chromatogram of a saponified solution of *p*-HATS after extraction into hexane and addition of α -TOH.

To further investigate the identity of the peak at 16.6 minutes, 2.42 pmol of α -TOH were added to a sample extracted in hexane after saponification and the mixture was analyzed using HPLC/ECD. The chromatogram obtained is shown in Figure 49. The detector signal due to α -TOH is significantly greater than the one in Figure 48. This showed that, indeed, α -TOH is a hydrolysis product of *p*-HATS.

CHAPTER 4

DISCUSSION

The purpose of this research was to investigate and compare the toxicity and uptake of TPGS and α -TS by RAW 264.7 and LNCaP cells. Both esters are hydrolyzed intracellularly to produce α -TOH. α -TS is also a hydrolysis product of TPGS. Cell viability measured by PI, CFDA and MTT assays indicated that RAW 264.7 macrophages are killed when exposed overnight to concentrations of TPGS at or greater than 12.4 μ M. LNCaP cells treated in similar experimental conditions show significant cell death with TPGS concentrations at or greater than 24.8 μ M. However, it is noted from Figure 30 that both cell lines start dying when treated overnight with initial concentrations of 12.4 μ M α -TS. Hence, 12.4 μ M of α -TS would kill RAW 264.7 or LNCaP cells macrophages after 24 hours but 12.4 μ M of TPGS would kill only RAW 264.7 macrophages after such time. These results suggest that α -TS might be more cytotoxic than TPGS.

From the results in Figure 30, it can be concluded that RAW 264.7 are more sensitive than LNCaP cells when both are treated for 24 hours with the same concentration of α -TS. This can be explained by the fact that macrophages contain high levels of esterases. This raises the question of the real cause of cell death observed. To determine whether cytotoxicity is due to TPGS and/or one of its hydrolysis products, the uptake and hydrolysis of TPGS and α -TS must be taken into consideration.

α -TOH, PEG 1000, and succinate do not cause cell death⁴². The cytotoxic substances in this study are, therefore, TPGS itself, α -TS or both. Table 4 shows that the tocopherol taken up by cells mostly remains as TPGS and/or α -TS. Percentages of cellular α -TOH are very low further reinforcing the notion that free tocopherol is not responsible for the observed toxicity. It is shown in Figures 31-34 that macrophages take up more TPGS or α -TS than LNCaP cells do. This explains their cell death at lower initial concentrations of TPGS. It can be said from all these facts that RAW 264.7 and LNCaP cells treated with TPGS die due to TPGS and /or α -TS, but not α -TOH.

In an attempt to distinguish which one of the two esters killed cells, an anilide derivative of α -TS, *p*-HATS was considered as an analytical tool. Unlike α -TS, *p*-HATS has a free hydroxyl group and can therefore be detected using HPLC/ECD. A sample containing TPGS and α -TS could be used as a starting reagent in order to synthesize *p*-HATS. Based on the assumption that only α -TS would react, measurement of *p*-HATS by HPLC would then give an indication of how much α -TS was in the starting material. This aspect was not further developed in this research; however, some critical properties of *p*-HATS were studied.

The data in Figure 38 indicate that 400 mV, the optimal potential for detection of vitamin E compounds, can also be used to detect *p*-HATS. The chromatograms in Figures 39 and 40 show that *p*-HA, 5, 7-DMT, *p*-HATS, and α -TOH elute from the column in the order $p\text{-HA} < 5, 7\text{-DMT} < p\text{-HATS} < \alpha\text{-TOH}$.

The extraction of *p*-HATS in hexane, octane, methylene chloride, and ethyl acetate were also carried out. Hexane and octane give a very low recover of *p*-HATS compared to the mobile phase. This can be explained by the fact that the amide side chain in *p*-HATS is highly polar compared to the PEG 1000 moiety in TPGS. Hexane and octane are straight hydrocarbon chains and both have a polarity index of 0.00⁴³. Therefore, even though they are suitable for the extraction of TPGS and α -TS, they do not solubilize *p*-HATS at high levels. Methylene chloride and ethyl acetate are two compounds with polarity indexes 3.1 and 4.4, respectively. They were both found to extract high levels of *p*-HATS, as can be seen from the response factors 0.6489 and 0.6355, respectively, compared to 0.6194 in the mobile phase. Ethyl acetate was shown to dry faster under nitrogen than methylene chloride and the background noise in Figure 44 was less than the one in Figure 43. Therefore, to extract *p*-HATS, ethyl acetate was the best solvent among the four that were evaluated.

In order to identify the hydrolysis product(s) of *p*-HATS, saponification of the ester with saturated KOH was carried out. Possible compounds include *p*-HA, α -TOH, succinate, and α -TS. The results from Figures 45 and 46 indicate that *p*-HA is produced in low amounts by the hydrolysis of *p*-HATS. The strong peak that elutes after 16.6 minutes after extraction in methylene chloride or hexane is an indication that the compound is not highly polar. Indeed, if the amide group was still part of the compound,

its recovery in hexane would be low. α -TS and succinate are not electroactive species. These facts suggest that α -TOH might be the compound that elutes after 16.6 minutes. This hypothesis is further confirmed by the fact that the detector signal is increased, in Figure 49, when extra α -TOH is added to the saponified sample. Therefore, α -TOH is a hydrolysis product of *p*-HATS. If carried out successfully, the use of a cell extract containing TPGS and α -TS as a starting material in the synthesis of *p*-HATS would reveal what levels of α -TS are left in the cells and confirm whether cytotoxicity is caused by TPGS alone or by a combination of both esters. The toxicity and uptake of TPGS by normal cells remain to be addressed.

CHAPTER 5

CONCLUSION

This research, which included the cellular toxicity and uptake of TPGS and α -TS as well as critical properties of *p*-HATS, gave the following results:

- a) Overnight treatment of RAW 264.7 macrophages with TPGS concentrations at or greater than 12.4 μ M cause cell death. LNCaP cells are killed under the same conditions with TPGS concentrations of at least 24.8 μ M. Both cell lines start dying when treated overnight with at least 12.4 μ M. These data suggest that α -TS is more cytotoxic than TPGS.
- b) RAW 264.7 are more sensitive than LNCaP cells when treated overnight with similar concentrations of α -TS.
- c) When both cell lines are incubated with 24.8 μ M TPGS or α -TS for 24 hours, higher concentrations of total tocopherol are obtained from TPGS than from α -TS.
- d) RAW 264.7 macrophages take up more TPGS or α -TS than LNCaP cells do.
- e) Cellular total tocopherol consists mainly of TPGS and/or α -TS. Very low levels of α -TOH are in the cell. These facts suggest that the observed cell death is due to TPGS and/or α -TS but not α -TOH.
- f) *p*-HATS is an electroactive species and can be detected effectively using HPLC/ECD.
- g) *P*-HATS can be detected using 400 mV, the oxidation potential for the detection of vitamin E compounds.
- h) The use of ethyl acetate as an extraction solvent gives a good recovery of *p*-HATS from samples.
- i) *p*-HA and α -TOH are hydrolysis product of *p*-HATS.

BIBLIOGRAPHY

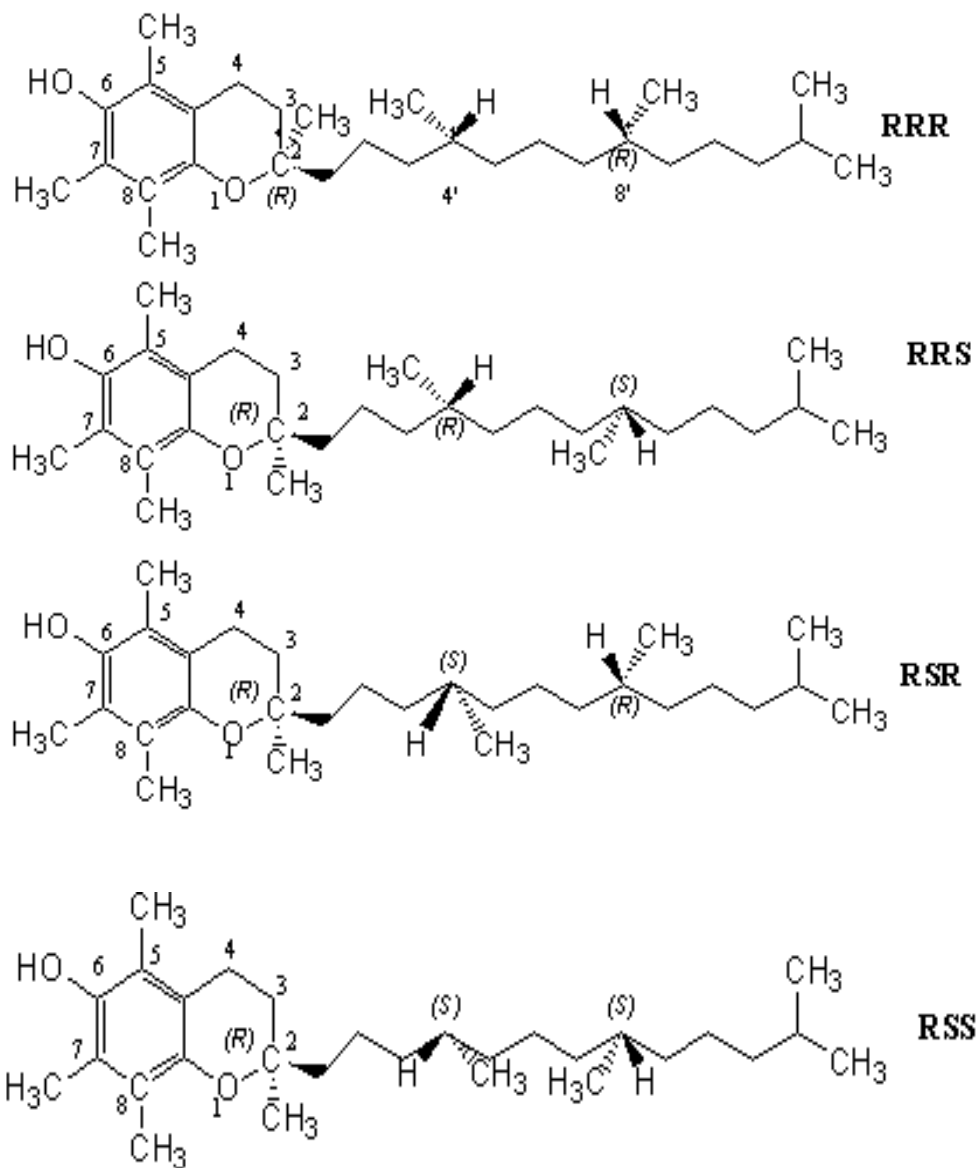
1. Andreas Papas. *The Vitamin E Factor: the miraculous antioxidant for the prevention and treatment of heart disease, cancer, and aging*; HarperCollins Publishers: New York, 1999.
2. Azzi, A; Stocker, A. *Progress in Lipid Research*.**2000**, 39, 3, 231-255.
3. Wagner, B; Buettner, G; Burns, P. *Archives of Biochemistry and Biophysics*. **1996**, 334, 2, 261-267.
4. Topinka, J; Binkova, B; Sram, R. J; Erin, A.N. *Mutation Research Letters*. **1989**, 225, 3, 131-136.
5. Kumarasamy, S; Aranganathan, S; Namasivayam, N. *Clinica Chimica Acta*. **2004**, 339,37-32
6. Van Der Logt, E. M. J; Roelofs, H.M. J; Wobbes, T; Nagengast, F. M; Peters, W. H. M. *Free Radical Biology and Medicine*. **2005**, 39, 2, 182-187.
7. Monte S. W; Wians, F. H., Jr. *Clinica Chimica Acta*.**2003**, 330, 1-2, 57-83.
8. Heinonen, O. P; Albanes, J; Virtamo *et al. J Natl Cancer Inst*.**1998**, 90, 440-446.
9. Lieberman, R. *Urology*. **2001**, 57, 4, 224-229.
10. Wu, S.H.; Hopkins, W. *Pharm Tech*.**1999**, 23, 10
11. The Doctor's Lounge.net. Free radical mechanisms in cancer formation. <http://www.thedoctorslounge.net/oncolounge/articles/oxidcar/> (accessed 06/08/05).
12. Malins, D. C; Johnson, P.M; Wheeler, T.M; Barker, E.A; Polissar, N.L; Vinson, M.A. *Cancer Research*.**2001**, 61, 6025-6028/
13. Malins, D.C; Polissar, N.L; Gunselman, S.J. *Proc. Natl. Acad. Sci. U. S. A.* **1997**, 94, 259-264.
14. Bokov, A; Chaudhuri, A; Richardson, A. *Mechanisms of Ageing and Developmen.*, **2004**, 125, 10-11,811-826. Association of Online Cancer Resources.
15. Sies, H. *Exp. Physiol.* **1997**, 82, 291-295.
16. Sies, H. *Am. J. Med.* **1991**, 91, 31S-38S.

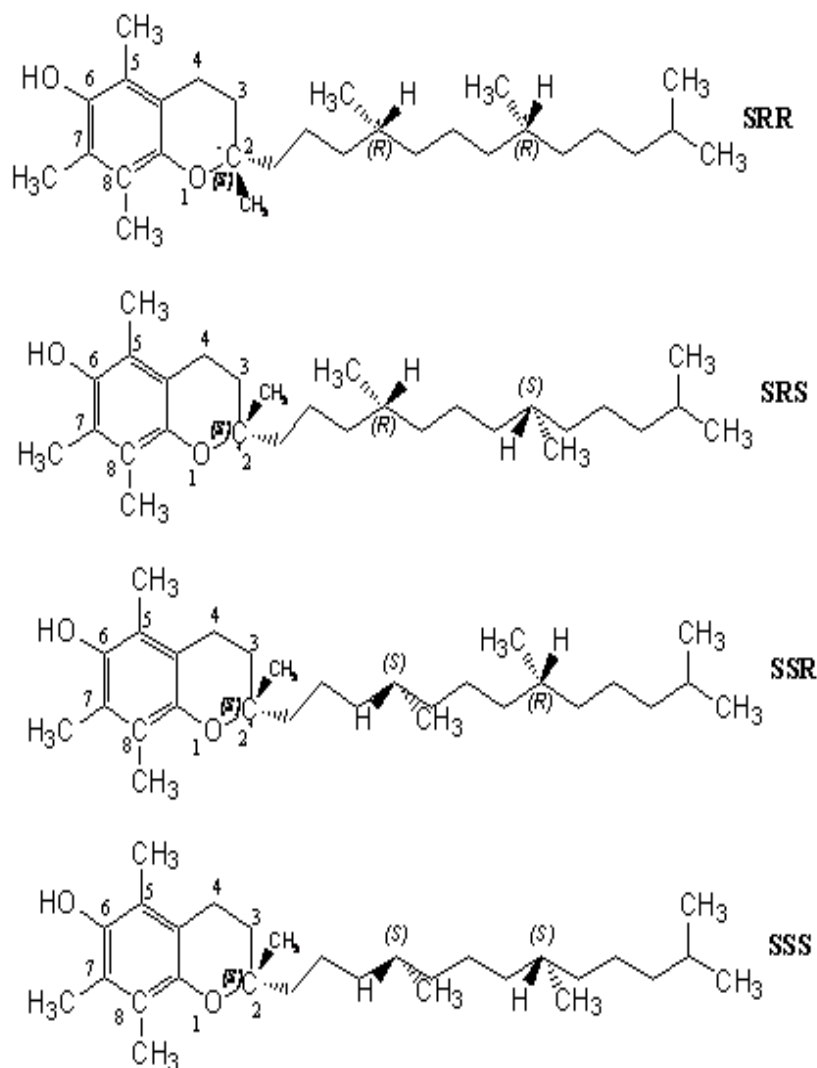
17. Yamada, K; Shoji, M; Mori, T; Ueyama, N; Matsuo, S; Oka, K; Nishiyama ; M. Sugano. *In Vitro Cell. Dev. Biol. Anim.* **1999**, 35, 169–174.
18. Fremont, L; Gozzelino, M.T; Linard, A. *Lipids* **2000**, 35, 991–999.
19. Liu, Z; Ma, L.P; Zhou, B; Yang, L; Liu, Z.L. *Chem. Phys. Lipids.* **2000**, 106, 53–63.
20. Fisher, A. E. O; Naughton, D.P. *Bioorganic & Medicinal Chemistry Letters.* **2003**, 13, 10, 1733-1735.
21. The Doctor's Lounge.net. Antioxidants, nature and chemistry. <http://www.thedoctorslounge.net/medlounge/articles/antioxidants/> (accessed 06/08/05)
22. Fleshner, N.E; Kucuk, O. *Urology.* **2001**, 57, 90–94.
23. Reddy, L; Odhav, B; Bhoola, K.D. *Pharmacology & Therapeutics.* **2003**, 99, 1, 1-13.
24. Vaya, J; Aviram, M. Nutritional Antioxidants: Mechanisms of action, Analyses of Activities and Medical Applications. <http://www.bentham.org>
25. De Leiris, J. Biochemistry of free radicals. <http://www.heartandmetabolism.org/issues/HM19/hm19refrcorner.asp> (accessed 06/08/05)
26. Li, X; Huang, J; May, J.M. *Biochemical and Biophysical Research Communications.* **2003**, 305, 3, 656-661.
27. Dallner, G; Sindelar, P.J. *Free Radical Biology and Medicine.* **2000**, 29, 3-4, 285-294.
28. Prevention of prostate cancer. <http://www.acor.org/cnet/305029.html> (accessed 06/08/05).
29. Weinstein, S.J; Wright, E.M; Pietinen, P; King, I; Tan, C; Taylor, P.R; Virtamo, J; Albanes, D. *Journal of the National Cancer Institut.* , 2005, 97, 5, 396-399.
30. Israel, K; Yu, W; Sanders, B.G; Kline, K. *Nutrition and Cancer.* **2000**, 36, 1, 90-100.
31. ESA. Inc. *Coulochem®II Operating manual*; 50-6479; Chelmsford, MA, U.S.A. **1996**, pp3-9

APPENDIX

Stereoisomers of RRR- α -Tocopherol

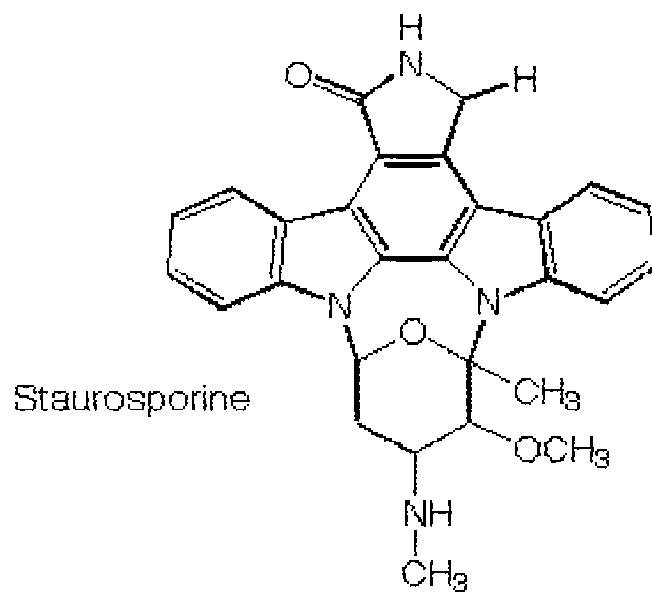
Chemical structures of the 8 stereoisomeric forms of tocopherol are shown below:





Staurosporine

This is a microbial alkaloid isolated from *Streptomyces* species. It has a strong toxic effect on the growth of various mammalian cells and, as such, was used in cell viability experiments as positive control. The chemical structure of staurosporine is shown below:



Structure of staurosporine

VITA

CHRISTELLE KOMGUEM KAMGA

Personal Data: Date of Birth: January 01, 1984
Place of Birth: Douala, Cameroon, Africa
Marital Status: Single

Education: University of Buea, Cameroon, Africa
Chemistry, B.S., 2002
East Tennessee State University, Johnson City, Tennessee;
Chemistry, MS., 2005

Professional
Experience: Graduate Assistant, East Tennessee State University, College of
Arts and Sciences, 2003-2005
Research Assistant, East Tennessee State University, James H. Quillen
College of Medicine, 05-08(2004&2005)